Materials Today Energy 7 (2018) 58–79

Contents lists available at ScienceDirect

Materials Today Energy

journal homepage: www.journals.elsevier.com/materials-today-energy/

A cross-disciplinary overview of naturally derived materials for electrochemical energy storage

Mengyao Gao [a, b, 1], Shu-Yuan Pan [b, 1], Wen-Chang Chen [a, *], Pen-Chi Chiang [b, c, **]

[a] Department of Chemical Engineering, National Taiwan University, Taiwan
[b] Carbon Cycle Research Center, National Taiwan University, Taiwan
[c] Graduate Institute of Environmental Engineering, National Taiwan University, Taiwan

ARTICLE INFO

Article history:
Received 17 October 2017
Received in revised form
22 November 2017
Accepted 13 December 2017
Available online 21 December 2017

Keywords:
Plant-based biomass
Rechargeable batteries
Supercapacitors
Environmental benefits
Circular economy

ABSTRACT

Due to global climate change and resource shortages, significant attention has been focused on exploiting environmentally friendly materials, such as naturally derived materials (e.g., biomass), for electrochemical energy storage to achieve a circular economy. One current area of research focus is bionics, which is a promising strategy to make materials with three-dimensional ordered structures that offer multiple contributions to bulk electrochemical properties. To develop high-performance energy storage devices, this article first reviews advances in the design and synthesis of nanostructured materials from plant-based biomass. The challenges and limitations on achieving high-performance rechargeable batteries are also illustrated and discussed from the materials design point of view. Then, from the perspective of chemical engineering, the performance of porous carbon from plant-based biomass for various applications is elucidated. Comprehensive performance evaluations on the relationship between the structure and electrochemical properties of biomass-derived materials are performed and summarized. Finally, the environmental benefits and impacts of electrochemical energy storage devices using biomass are discussed. From the perspective of environmental engineering, the recycling and reuse of metal components from spent batteries through the concept of green chemistry are presented. This article should be considered a pioneering review providing a holistic overview of electrochemical energy storage devices using plant-based biomass from a cross-disciplinary perspective that encompasses on materials science, chemical engineering and environmental engineering.

© 2017 Elsevier Ltd. All rights reserved.

1. Introduction

1.1. Technologies for electrochemical energy storage (EES)

Nowadays, a new energy economy based on a cheap and sustainable energy supply and storage is emerging. Electrical energy storage can provide a wide range of services and/or applications, including portable electronics, hybrid electric vehicle (EV), and devices for renewable energy storage from solar and wind [1–4]. State-of-the-art electrochemical energy storage (EES) devices, such as lithium ion batteries (LIBs), lithium-sulfur batteries (LiSBs) and supercapacitors, have great potential to play a significant role in the large-scale energy storage field. For instance, low-carbon, eco-friendly and cost-effective public transport systems are becoming more and more significant in our daily life. Population and economic growth are leading to a significant increase in global energy consumption. Along the way, lithium-based batteries, such as LIBs and LiSBs, have become a key enabling technology for energy storage and are expected to be widely used in significant quantities for automotive propulsion [5] and the EV industry [6]. The global vehicle market is expected to reach about 180 million sales by 2045, where ~100 million sales would come from electric battery vehicles [7]. Therefore, it is crucial to develop lithium-based batteries with superior electrochemical performances, including higher energy density, higher power density, and longer life. Also, the sustainability and safety of the materials should be the focus in this race for high performance batteries.

In general, EES devices are composed of an anode, a cathode, an electrolyte and a separator separating the two electrodes. For the

* Corresponding author. No 1, Sec 4, Roosevelt Rd., Taipei, 10617, Taiwan.
** Corresponding author. No 71, Chou-Shan Rd., Taipei, 10673, Taiwan.
E-mail addresses: chenwc@ntu.edu.tw (W.-C. Chen), pcchiang@ntu.edu.tw (P.-C. Chiang).
[1] These authors contributed equally to this work and should be considered co-first authors.

https://doi.org/10.1016/j.mtener.2017.12.005
2468-6069/© 2017 Elsevier Ltd. All rights reserved.

electrodes, alloy and conversion materials with high specific capacity such as silicon, sulfur, and conversion metal oxides have the most promise to increase the energy density of LIBs [8]. The main components of electrode in existing LIBs, such as $LiCoO_2$ and $LiMn_2O_4$, are produced not from renewable materials but from natural ores, which would gradually become scarcer. To improve the energy density of LIBs for meeting the requirement of the 500 km range between charges for EVs and grid energy storage, alternative materials with reduced cost and increased capacity are needed.

1.2. Carbon materials derived from natural biomass for energy applications

Elemental carbon, also known as black carbon, is a non-metallic material usually handled in three forms: graphite (crystalline), diamond (crystalline), and amorphous carbon. A number of carbon-based materials, such as activated carbon (AC), pyrolytic carbon, carbon black, graphite fiber, glassy carbon and carbon whiskers have been applied in electrochemistry for decades. Porous carbon materials have attracted considerable attention since the 1960's because of their wide variety of scientific and technological applications [9]. In general, porous carbons are prepared by carbonization of organic felts or fibers (e.g., cellulose) under inert atmosphere or under reducing conditions. Until now, numerous new techniques for preparing porous carbon materials, including composites, functionalization, encapsulation, doping and intercalation, have been introduced in the field of electrochemistry [10–12].

Novel porous carbon materials have attracted considerable attention as applied in adsorbents, gas storage, catalysts, battery electrodes, and supercapacitors. Porous carbon materials have proven to be the most promising electrodes in LIBs because of their low cost, easy accessibility and processability. However, most sources of current porous carbon materials are non-renewable fossil-based carbon. In other words, it is urgent to develop renewable derivatives and/or products via the waste-to-resource concept as economic viable and environmentally friendly approaches to preparing ACs. Inspired by nature, the chemistry of life with its virtually unlimited and incredible reaction mechanisms with diverse properties and chemical compositions have captured attention.

Biomass materials are mainly derived from natural plants or living organisms (e.g., animals), which are considered as earth-abundant renewable sources. However, biomass may result in the greenhouse effect, fog and other detrimental environmental impacts if it is incinerated [13,14]. For plant-derived biomass, apart from agricultural resides, the disposal of forest byproducts usually involves burning, which causes severe air pollution. Therefore, employing plant-derived biomass to establish the waste-to-resource supply chain can not only reduce the utilization of fossil fuels but also achieve the goals of greenhouse gas (GHG) emission reduction [15,16]. Waste biomass is an intriguing and promising resource for materials synthesis, since it is produced in large quantities from agriculture and industry. According to the United Nations, global estimated biomass production is 146 billion tons per year, accounting for 35% of primary energy consumption in developing countries, and raising the world total to 14% of primary energy consumption [17]. To achieve the goals of social sustainability and environmental friendliness, various types of plant-derived biomass can be used to prepare porous carbon materials for such applications as electrode materials in energy storage devices, including LIBs [18], LiSBs [19,20], and supercapacitors [21]. Various types of biomass-based materials, such as porous ACs, have been successfully synthesized via pretreatment [22,23]. In addition, waste biomass can be converted to heat via numerous technologies such as combustion and pyrolysis, or be used indirectly after conversion to various forms of biofuel [24]. For instance, pyrolysis is a thermochemical conversion technology which removes the moisture and volatile matter contents of the biomass in the absence of oxygen to generate bio-char, bio-oil and bio-gas products [25].

1.3. Establishment of a circular economy toward sustainable development

New energy storage technologies are imperative to realize a sustainable energy future that is compatible with sustainable development goals (SDGs). For instance, the development of environmentally sustainable and rechargeable batteries should be beneficial to the field of energy storage in such applications as automotive electric vehicles, mobile devices, and laptops. In particular, this can ensure the eradication of extreme poverty (SDG-1) and the creation of decent work and economic growth (SGD-8) [26], as well as playing a key role for affordable and clean energy (SDG-7), and industry, innovation and infrastructure (SDG-9). The creation and use of sustainable materials for batteries must involve the synthesis of novel electrode materials and electrolytes with high efficiency and low cost by materials scientists and engineers. Abundant and inexpensive biomass should be a suitable alternative to raw materials for electrode synthesis and production in batteries. In fact, materials can be harvested from biomass resources with proper design and thermally disposed to achieve low environmental impacts [27]. Meanwhile, the huge demand has motivated scientific and technological efforts dedicated to developing a battery recycling system for achieving a circular economy system (CES).

For instance, LIBs are currently classified as Class 9 miscellaneous hazardous materials under United States regulations (40 CFR 173.21(c) [28], which should be properly managed and treated once they reach the end-of-life stage. Therefore, the establishment of a waste-to-resource supply chain should provide a method of overcoming the barriers of resource demand, waste management, and GHG emissions to achieve a CES [29]. On the other hand, from a life-cycle point of view, significant environmental impacts can occur from the raw material extraction stage in the mining and processing of ores. For instance, obtaining one ton of lithium requires approximately 250 tons of mineral ore or 750 tons of brine, compared with 28 tons of used batteries [30]. These adverse impacts can be avoided if the materials can be recycled [31].

1.4. Objectives of review

This review presents a pioneering review on the application of plant-based biomass for EES devices from a cross-disciplinary perspective that encompasses materials science, chemical engineering and environmental engineering. The fundamental structures and chemistries of plant-derived nanostructured materials are essential for a wide range of existing and new enabling technologies. It is also imperative for realizing a sustainable energy future that is compatible with the SDGs. In this review, the fundamental properties, e.g., structures, of plant-derived nanostructured materials are first reviewed for designing and manufacturing EES products from the perspective of materials science. Then, the performance of porous carbon obtained from plant-based biomass in various applications, such as rechargeable batteries and supercapacitors, are comprehensively evaluated and discussed. Furthermore, the perspective of environmental engineering is combined with chemical engineering and materials engineering to reveal the importance and significance of green chemistry and recycling technologies for spent batteries. Lastly,

based on the progress made with the aforementioned strategies, future research directions for improvement and practical utilization for EES devices are presented.

2. Design and synthesis of carbon materials from plant-derived biomass

Exploitation of plant-derived biomass plays an imperative role in establishing sustainable and renewable systems toward a circular economy. Plants, mainly comprise carbon (C), hydrogen (H) and oxygen (O), are natural organisms that can be converted into green energy and materials such as low-cost carbons [32]. Numerous plant-derived biomass, such as coconut shells [33,34], rubber-seed shells [35], bamboo [36], rice husks [37,38], corncob husks [39], banana peels [40,41], cassava peels [42], pomelo peels [43,44], palm-tree cobs [45], plum kernels [46], jute fibers [47], nutshells [48], ramie [49,50], bagasse [51], olive bagasse [52], olive and peach stones [53,54], date stones [55], date fronds [56], date pits [57], and wood/cotton residues [58], can be used as the precursor to prepare porous carbon materials. In this part, the preparation method, design criteria and functionalization of porous carbons from plant-derived biomass are illustrated.

2.1. Preparation of porous carbon materials

Physical and chemical activation have been extensively employed before carbonization to fabricate the pore network in carbon materials [59,60]. Physical activation (so-called gas activation) is oxidizing carbon materials in gasifying agents to generate porosity, accompanied by the carbonization of precursors in an inert atmosphere [61]. Chemical activation, on the other hand, is usually performed via impregnation with chemicals and dehydrating agents at a specific proportion [62]. Physical activation is an environmentally benign process since it uses gaseous agents for activation without generating wastewater. However, it usually takes a longer activation time, and therefore greater thermal energy, to produce microporous AC, compared to chemical activation. In this part, the principles of physical and chemical activation are illustrated.

2.1.1. Physical activation

In physical activation, the precursor (source material) is developed into porous carbon by hot gas. It involves one or a combination of the following processes: (1) carbonization: carbon precursors are pyrolyzed at a proper temperature (500–1000 °C), usually in an inert atmosphere such as argon and nitrogen; and (2) thermal activation: the as–prepared materials are exposed to oxidizing atmospheres, such as air, steam, O_2 and CO_2, at an elevated temperature above 250 °C (usually 600–1200 °C). ACs with high surface areas and porosity can contribute to excellent electrochemical performance [63]. For instance, Su, et al. [64] created ACs via an adiabatic expansion at the state of thermal degradation followed by carbonization to create a microporous structure of ACs. However, physical activation would reduce both the particle and microdomain sizes of ACs, which may be disadvantageous to the performance of materials depending on the types of applications.

2.1.2. Chemical activation

In chemical activation, prior to carbonization, the precursor is impregnated with certain chemicals, i.e., dehydrating agents, and then carbonized at temperatures from 450 to 900 °C. Different types of biomass, such as willow catkin [65], elm samara [66], fungus [67], cotton [68], bamboo [69], shiitake mushrooms [70], elm samara [66], corn cobs [71], broad beans [72], sunflower seed shells [73], fallen leaves [74], fruit bunches [75], cherry stones [76], apricot shells [77], rice husks [78], coffee grounds [79], ramie [80], and pomelo mesocarps [81], have been successfully used with dehydration agents during the chemical activation stage. It is noted that chemical activation could introduce oxygen functionalities in the carbon surface.

Typical dehydrating agents (or activating agents) include potassium hydroxide (KOH), sodium hydroxide (NaOH), sodium carbonate (Na_2CO_3), magnesium chloride ($MgCl_2$), phosphoric acid (H_3PO_4) and zinc chloride ($ZnCl_2$). Fig. 1 shows the BET surface area of ACs via chemical activation through KOH, NaOH, $ZnCl_2$ and $CaCl_2$ agents at various temperatures. Chemical activation can promote the surface area of porous carbons over 2000 $m^2\ g^{-1}$, even up to 3400 $m^2\ g^{-1}$ in the case of KOH activation [82]. In addition, large pore volumes are mainly made up of micropores and some small mesopores. It is noted that chemical activation exhibits relatively low activation temperatures, short activation time, high yields and high specific surface area over physical activation. However, washing processes are required due to the corrosion caused by the applied chemicals. It has been found that KOH merely widens micropores to more heterogeneous micropores, whereas $ZnCl_2$ develops both wide micropores and low mesopores, and H_3PO_4 developed large mesopores and even macropores [54].

In the KOH activation process, for instance, it is transformed in K_2O via the dehydration reaction under 700 K, as shown in Eq. (1):

$$2\ KOH_{(l)} \rightarrow K_2O_{(s)} + H_2O_{(g)} \quad (1)$$

The carbon sources would be consumed by the reaction between C and H_2O with the production of CO_2 and H_2 gases, as shown in Eqs. (2) and (3):

$$C_{(s)} + H_2O_{(g)} \rightarrow CO_{(g)} + H_{2(g)} \quad (2)$$

$$CO_{(g)} + H_2O_{(g)} \rightarrow CO_{2(g)} + H_{2(g)} \quad (3)$$

Then K_2CO_3 can be formed via the reaction between K_2O and CO_2:

$$K_2O_{(s)} + CO_{2(g)} \rightarrow K_2CO_{3(s)} \quad (4)$$

When the temperature increases to 900 K, KOH is completely consumed, leading to the formation of metallic potassium, as

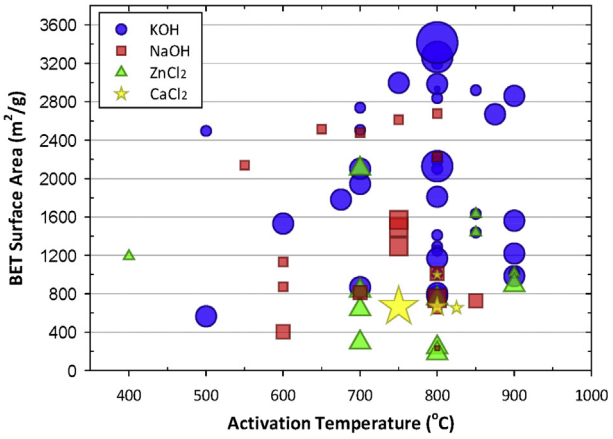

Fig. 1. BET surface area of plant-derived porous carbons through KOH, NaOH, $ZnCl_2$ and $CaCl_2$ agents at various temperatures. Available information in the literature [40,44,66,68,70,73,76,82–109] was gathered and summarized.

shown in Eq. (5). The formed metallic potassium may diffuse into the carbon matrix, resulting in the expansion of carbon lattices.

$$6\ KOH_{(l)} + 2\ C_{(s)} \rightarrow 2\ K_{(s)} + 3\ H_{2(g)} + 2\ K_2CO_{3(s)} \quad (5)$$

When temperature is over 1000 K, K_2CO_3 starts to decompose to K_2O and CO_2, and it completely disappeared at ~1100 K, as shown in Eq. (6).

$$K_2CO_{3(s)} \rightarrow K_2O_{(s)} + CO_{2(g)} \quad (6)$$

Since the pyrolysis and activation step proceeds simultaneously with chemical activation, chemical activation is usually performed in a single step at 700–1200 °C combining carbonization and activation [110]. It is noted that KOH activation can induce homogeneous pore development for carbon particles without changing the sizes of the microdomains or particles. However, steam activation might cause inhomogeneous gasification from the outer surface of the carbon particles and microdomains.

Pore development mechanisms between physical and chemical activation processes (Fig. 2a) was compared by Miyawaki's group [111]. In the case of KOH activation, uniform pore development for microdomains consisting of carbon particles can be efficiently achieved without apparent changes in morphology (Fig. 2b). In the case of steam activation, in contrast, micropore development was nearly linear over the activation temperature range. As shown in Fig. 2c, the microdomain size would be significantly reduced depending on the temperature of activation, from 5.6 nm (at 700 °C) to 2.9 nm (at 900 °C). Moreover, ACs prepared by physical activation (Fig. 2d) exhibited lower specific surface areas and lower yields than those prepared by chemical activation (Fig. 2e).

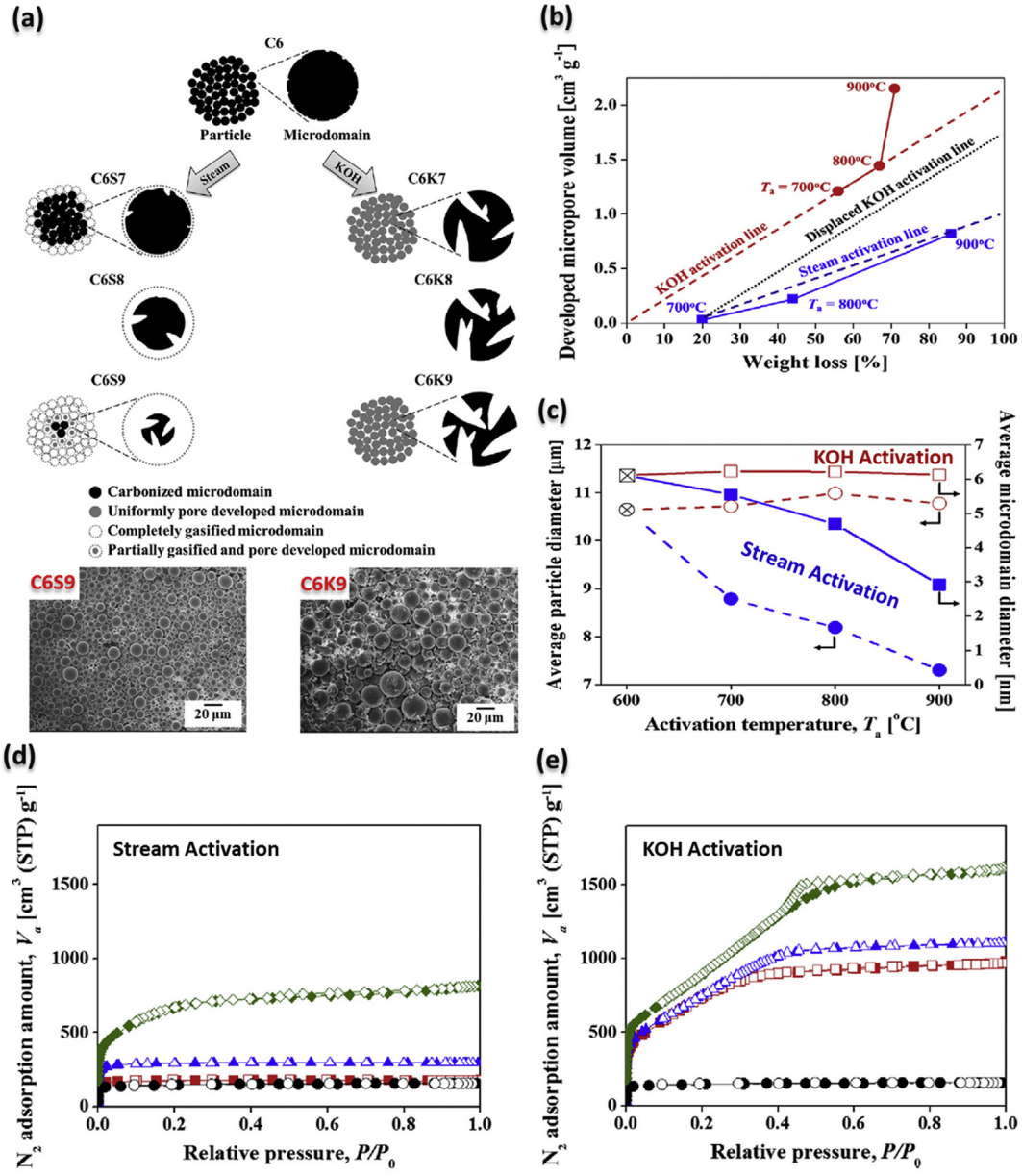

Fig. 2. (a) Structural mechanism model of pore development for steam- and KOH–ACs. (b) Relationship between weight loss and developed micropore volume of (square) steam- and (circle) KOH–ACs prepared at different activation temperatures (T_a); (c) Change of average sizes of (circle) particles and (square) microdomains by steam (solid symbol) and KOH (open symbol) activations depending on activation temperature. N_2 adsorption (solid symbol)/desorption (open symbol) isotherms at 77 K for (d) steam- and (e) KOH–ACs. Adapted from the literature [111].

2.2. Design criteria of carbonization/activation processes

Conventionally, porous ACs with high surface area and porosity are commonly used as adsorbents in environmental engineering, e.g., the removal of organic pollutants from flue air and/or wastewater streams in unit processes. According to the International Union of Pure and Applied Chemistry (IUPAC), pores of a material can be classified into three groups: micropores (diameter, $d < 2$ nm), mesopores ($2 \text{ nm} < d < 50$ nm), and macropores ($d > 50$ nm). For typical ACs, the specific surface areas are in the range of 800–2300 $m^2 g^{-1}$, while the mesopore surface areas are 10–200 $m^2 g^{-1}$. The mesopore volumes of ACs vary between 0.1 and 0.2 $cm^3 g^{-1}$, even up to 0.5 $cm^3 g^{-1}$ for special cases [112].

Utilizing biomass for synthesizing and manufacturing porous ACs for EES applications has become strategically attractive [113]. Carbonization converts organic substances in biomass into carbon or carbon-containing residues through pyrolysis or destructive distillation. The conversion performance depends on the operating conditions, such as temperature [114,115], heating rate [116,117], residence time [118,119], reactor configuration [119], and feedstock type [120]. For thermal activation, it is recognized that CO_2 can be applied for generating microporosity [55], while steam can produce a wide distribution of micropores and mesopores [121].

Date pits constitute approximately 10% by weight of the fruit, with carbohydrates as the major components of the pits. Porous carbon can be produced from Algerian date stones via pyrolysis (physical activation) at various activation/carbonization temperatures from 700 to 1000 °C in a fixed-bed reactor [56]. The BET surface area is 1094 $m^2 g^{-1}$, pore volume is 0.44 $cm^3 g^{-1}$, pore size is 16.09 Å, and yield is 18.8%. The lignocellulosic composition promotes the preparation of ACs from their precursors [122,123].

Low-cost carbon materials with interconnected, multichannel, and porous structures could be carbonized at high temperatures under a nitrogen atmosphere. Hameed et al. [124] converts plant-derived biomass (i.e., bamboo) to ACs by chemical activation with CO_2 and KOH as the activating agents at 850 °C for 2 h. During the hydrothermal process, the lignin segment between neighboring bamboo fibers gradually dissolves into the KOH solution at an elevated temperature. This approach can promote electrolyte access and ion diffusion, which makes plant-derived carbon materials suitable for electrochemical applications, such as LiSBs [125], supercapacitors [89,126], and fuel cells [127]. Similarly, an annealing process was developed for preparing porous biochar to create a microporous structure, boost surface area and enhance electronic conductivity [125].

Different pore sizes can be tailored by varying the temperatures of the activation process. When the carbonization temperature increases, the pore contraction process occurs due to the increase in temperature. Fig. 3 elucidates the structural changes in the pyrolytic carbons at different temperatures. Low-temperature pyrolysis would form disordered carbons with mesopores containing a relatively large amount of defects, while high-temperature would result in partially ordered carbons with cylindrical mesopores and micropores through the stacking of less defective graphene layers.

Since it offers passages to exchange between neighboring fibers, the originally natural nanostructures (e.g., cellulose and lignin) in biomass can supply additional access to the inside of microtubes and thus shorten the distances for ionic diffusion. Tubular cellulose fibers (for instance, about 60% in total mass of bamboo) serve as nutrient and water transport corridors between the root and the leaves. The role of lignin (10–20% in total mass), a sort of 3D highly cross-linked polyphenolic polymer, is to bind these fibers together [129]. Tubular, with lots of nanosized holes or cavities on the wall, could provide large inner surface areas and enrich the electrochemically active sites, which is preferable for energy storage applications such as LIBs and supercapacitors [129].

2.3. Functionalization of porous carbons

Surface functionalization or heteroatom doping can introduce chemical functional groups to the surface of materials. Heteroatom doping (surface functional groups) is an effective strategy to enhance the electrochemical activity of carbon materials such as sulfur-carbon composite cathodes [130–132]. Conventionally, template synthesis roughly involves the use of a structure-directing reagent, which requires the development of alternative fabrication approaches to produce high performance materials to meet industrial requirements [133]. In contrast, the development of functional nanostructures in a material usually involves expensive chemicals and elaborate processing, which presenting a great challenge for wide and low-cost implementation.

Functionalization, e.g., covalent attachment, adsorption, deposition, use of redox mediators as electrode modifiers, in-situ

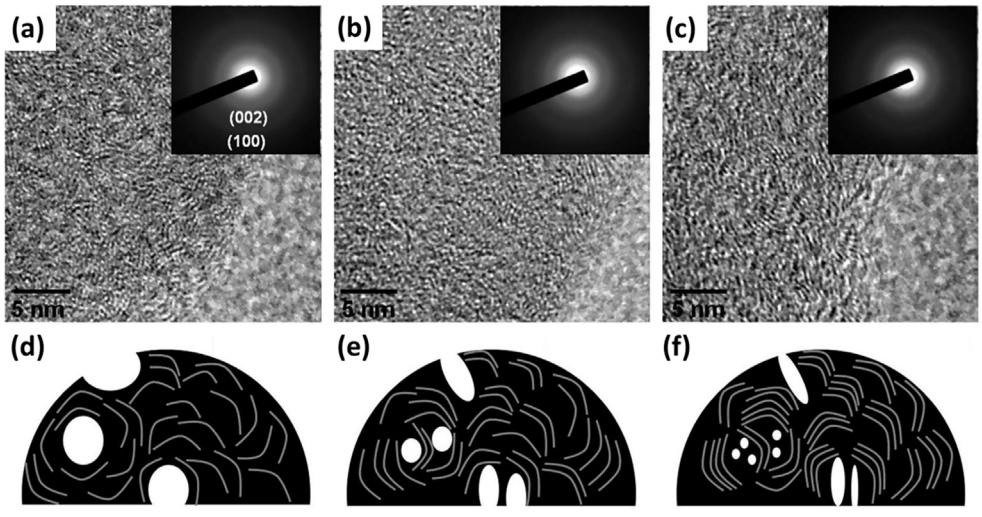

Fig. 3. TEM images of porous carbons pyrolyzed at (a) 700 °C, (b) 800 °C, and (c) 900 °C. Schematic illustrations of physical characterization for pyrolyzed carbons at (d) 700 °C, (e) 800 °C, and (f) 900 °C. Adapted from the literature [128].

functionalization of self-assembled monolayers, and electro-polymerization, can increase the catalytic ability of carbon electrodes toward selected processes. Two methods have typically been employed to promote the formation of covalent bonds during carbon functionalization [9]: (1) direct electrochemical oxidation through the application of a sufficiently positive oxidizing potential, high enough to produce oxygen functional groups on the carbon surface; and (2) electrochemically assisted reaction with a functionalizing substrate. For instance, the fabrication process of N-doped hierarchically porous carbon materials (N–HPCMs) through a hybrid dual-template method is shown in Fig. 4a. N (nitrogen) and B (boron) have similar molecular sizes and valence electron numbers to carbon. Fig. 4b and c illustrate the CO_2 sorption isotherms of the N–HPCMs and direct carbonization of banana peels, respectively. The results indicate that N–HPCMs exhibit a higher micropores volume due to the abundant nitrogen content. N is an attractive doped heteroatom to improve the carbon electrical conductivity and carbon wettability, restrain the diffusion of soluble polysulfides, and retards the shuttle effect in batteries [134].

The physico-chemical properties of ACs depend on not only the surface structure and porosity of precursors but also heteroatoms built in their structure. N-containing carbon has attracted great interests because of its excellent performance in applications such as CO_2 capture [135], removal of contaminants from gas and liquid phases [136], environmental protection [137], catalysts and catalyst supports [138], and supercapacitors, fuel cells and batteries [139]. There are mainly four types of N-functional groups, pyridinic (N1), pyrrolic (N2), quaternary groups (N3) and pyridine–N–oxide groups (N4). The content of pyridinic- and pyrrolic-like N atoms doped within the AC plays a critical role in the oxygen reduction reaction [140,141].

Being green, cheap and sustainable, N-containing ACs by hydrothermal treatment of amino containing carbohydrates synthesis is favorable for catalysis, adsorption and energy storage devices [137]. An environmentally friendly procedure to synthesize N- and P-doped porous carbons by 46% yield of coconut shell residues was introduced by Borghei et al. [33]. The synthesis method involved a single-step activation with phosphoric acid to achieve a high surface area (i.e., ~1215 $m^2\ g^{-1}$) and pore volume (i.e., ~1.15 $cm^3\ g^{-1}$ with 72% mesopores). Thus, the obtained materials are suitable as a cathode catalyst for alkaline fuel cells due to their great electrocatalytic activity.

N-doped nanoporous carbon nanosheets (NCS) from the Typha orientalis (a kind of plant) were formed in ammonia gas (NH_3) via a hydrothermal process [142]. The as–obtained fibers were ruptured and fractured to form the NCS, where NH_3 was used as the nitrogen source to form the N-doped carbons. In this process, numerous micropores can be generated by the production of a small quantity of Typha orientalis oil from the NCS and NH_3 etching of the carbon. The process chemistry for NH_3 etching of the carbon material can be described as Eqs. (7) and (8):

$$2\ NH_{3(g)} \rightarrow N_{2(g)} + 3\ H_{2(g)} \quad (7)$$

$$C_{(s)} + 2\ H_{2(g)} \rightarrow CH_{4(g)} \quad (8)$$

Furthermore, pomelo peel was used to fabricate H_3PO_4-activated carbon materials via pyrolysis at 700 °C in a N_2 atmosphere [143]. The obtained carbon materials have a 3D connected porous structure with a specific surface area (SSA) of 1272 $m^2\ g^{-1}$. According to the functional group analysis by XPS, O-containing functional groups could lead to a surface redox reaction between C–O functional groups. In addition, both N- and O-containing functional groups are beneficial to boost the electrochemical performance of the carbon-based anodes, in terms of electronic conductivity and reactivity.

2.4. Types of plant-derived precursor for porous carbons

Porous carbon, due to their relatively low inorganic content and relatively high volatile content, could be produced from an organic precursor and/or lignocellulosic materials. The non-renewable and expensive carbon precursors (such as coals, petroleum, polyacrylonitrile and phenolic resins), as well as the complex manufacturing processes associated with these sources restrict their large-scale applications. In contrast, being simple, scalable, cost-effective and environmentally friendly, plant-

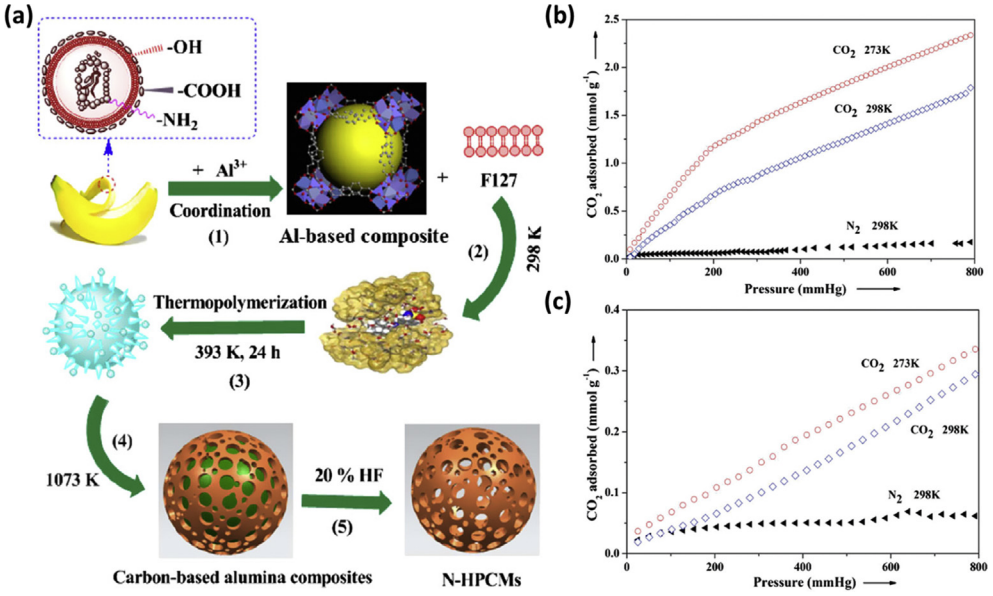

Fig. 4. (a) Fabrication of N-doped hierarchically porous carbon materials (N–HPCMs) through a hybrid dual-template method. CO_2 adsorption isotherms at 273 and 298 K and N_2 adsorption isotherms at 298 K for (b) N–HPCMs and (c) direct carbonization of banana peels. Adapted from the literature [134].

Table 1
Characteristic of plant-derived porous carbons via various Activation methods.[a]

Biomass materials	Activation method	Thermal procedure	Temperature (°C)		β (°C /min)	BET (m^2 g^{-1})	Pore volume (cm^3 g^{-1})		D_p (nm)	Reference
			T_{PC}	T_a			Total	Micropore		
Wood chips	Phys (CO)	One-step	–	800	10	133	0.21	0.05	6.2	[145]
Wood chips	Phys (CO_2)	One-step	–	800	10	590	0.34	0.18	3.4	[145]
Oil palm stone	Phys (CO_2)	One-step	–	850	10	1410	0.71	0.45	<2.0	[144]
Coal tar pitch	Phys (CO_2)	One-step	–	890	5	2487	–	0.86	–	[62]
Coconut shell	Phys (CO_2)	Two-step	600	900	10/50	1700	1.14	0.88	2.65	[146]
Palm petiole	Phys (CO_2)	Two-step	1000	850	5	546	0.24	0.23	0.6–1.2	[147]
Wood chips	Phys (N_2)	One-step	–	800	10	160	0.24	0.06	6.0	[145]
Coconut shell	Phys (N_2)	Two-step	250–350	850	5	663	0.23	–	1.39	[64]
Coconut shell	Che (H_3PO_4)	One-step	–	600	–	902	–	–	–	[148]
Rice straw	Che (H_3PO_4)	Two-step	350	600–800	5	377	0.32	0.20	1.0	[114]
Bamboo	Che (KOH)	One-step	–	800	–	776	–	0.33	0.75/1.58	[91]
Bamboo	Che (KOH)	One-step	–	800	–	808	–	–	–	[92]
Lotus seedpod	Che (KOH)	One-step	–	700–900	4	1813	1.05	0.22	3.3	[84]
Elm samara	Che (KOH)	One-step	–	700	–	1947	1.33	0.80	-	[66]
Wheat bran	Che (KOH)	One-step	–	800	5	2189	1.1	–	–	[86]
Peanut skin	Che (KOH)	One-step	–	800	5	2500	1.69	0.68	–	[94]
Cotton	Che (KOH)	One-step	–	900	5	1563	0.88	0.70	2.24	[68]
Pomelo peel	Che (KOH)	Two-step	500	600	–	1533	0.84	-	2.0–3.0	[44]
Mushroom	Che (KOH)	Two-step	500	800	5	2988	1.76	0.71	1.99	[70]
Banana peel	Che (KOH)	Two-step	700	800	3	2741	1.23	–	0.6–5.0	[40]
Bamboo	Che (KOH)	Two-step	700	800	10	1413	0.81	0.51	3.01	[89]
Seedpod shell	Che (KOH)	Two-step	400	850	3	2923	1.48	–	3.07	[93]
Rice husk	Che (KOH)	Two-step	300–500	650–850	–	3000	1.90	–	–	[95]
Coconut shell	Che ($ZnCl_2$)	One-step	–	800	10	2450	1.57	1.14	2.56	[112]
Rice husk	Che ($ZnCl_2$)	One-step	–	850	5	1442	0.71	0.65	–	[97]
Peanut shell	Che ($ZnCl_2$)	One-step	–	850	5	1634	1.39	0.25	3.39	[98]
Coffee bean	Che ($ZnCl_2$)	One-step	–	900	5	1019	0.48	0.21	2.0–4.0	[99]

[a] T_{PC} = precarbonization temp (°C); T_a = activation temp (°C); β = heating rate (°C/min); BET = BET surface area (m^2 g^{-1}); D_p = average pore width (nm).

derived biomass is attracting attention in EES applications. Table 1 presents the characteristic of plant-derived carbon materials via various activation methods for different EES applications. For both physical and chemical activation, there are two main thermal procedures for the preparation of AC: one-step and two-step. In the two-step procedure, carbon precursor is first carbonized in an inert atmosphere (so-called precarbonization) to generate rudimentary porosity, and then activated with oxidizing gas (i.e., physical activation) or with dehydrating chemicals (i.e., chemical activation) to further develop the surface area and porosity. In contrast, the one-step procedure eliminates the need for a separate carbonization process, and operated typically at a lower activation temperature. Therefore, the one-step procedure, compared to two-step procedure, exhibits additional advantages of low production costs in terms of energy and time savings [144]. It is necessary to explore cost-effective and renewable materials with precise structural, physical and chemical properties to meet industrial requirements. In this part, the characteristics of porous carbons prepared from various types of plant-derived biomass are illustrated.

2.4.1. Fruit peel-based materials

Different types of fruit peels, such as coconut shells, banana peels, shaddock peels, plum stones, watermelon peels, pomelo peels, and peach stones, can be used as starting materials for porous carbons. Coconut shell, a type of lignocellulosic residue in tropical areas, has attracted great attention for preparing porous AC because of its excellent natural structure with the high carbon content and low ash content [64]. Borghei, Laocharoen, Kibena-Põldsepp, Johansson, Campbell, Kauppinen, Tammeveski and Rojas [33] studied the pore changes from the raw shell, dried shell and carbonized shell to the AC stage. Based on the lignin contents (i.e., 30–49 wt%), the elemental compositions of coconut shells include high carbon content (i.e., 53–64 wt%) and low H/C and O/C ratios. The pore structure of coconut shell comprises cylinder-like tubes in layers of several flat sheets. At the charred stage, the pores maintain the cylindrical structure, while at the activated carbon stage, they deform significantly and lose their cylindrical character. Similarly, Zhang, et al. [149] prepared micro/mesoporosity coconut-shell-based porous carbons by a steam pyrolysis and activation process. The presence of mesopores in coconut-shell-based porous carbon improved the electrochemical performance. Conversion from raw coconut shells to porous carbons with a nitrogen BET surface area of 800–1500 m^2 g^{-1} and a mesopore volume of ~0.35 cm^3 g^{-1} have been extensively reported. Compared with porous carbons produced from polymers, plant-derived porous carbons exhibit the advantages of low cost and abundance in the acquisition of carbon precursors [149].

Banana peel, a common agricultural waste, represents 40% of the total weight. They have a porous structure formed by biopolymers, such as celluloses, hemicelluloses, pectins, lignins and proteins, in plant cell walls. Due not only to their pore structures but also to the carboxyl and hydroxyl groups on the surface of the pores, banana peel is known as a sorbent for cost-effective adsorption of phenolic compounds and heavy metals (such as zinc, copper, nickel, and chromium) from aqueous solution. For instance, the hydroxyl and carboxylic groups on the surface of pores can coordinate with zinc ions to form zinc complexes. Lv et al. [150] prepared porous AC from banana peel incorporating mesopores and micropores via pyrolysis followed by KOH activation. The unique self-supported hierarchical structure possesses a high SSA of 1650 m^2 g^{-1} and provides a more favorable path for electrolyte penetration and transportation.

Fig. 5a illustrates the synthetic process for the nitrogen-doped nanoporous carbon (NPC) electrodes. The dried shaddock peels were soaked in a saturated melamine solution for 10 min. The results indicated that the dried shaddock peels exhibited a continuous 3D fibrous structure with pore sizes ranging from 100 to 200 μm. The surface area and total pore volume of NPC carbonized at 900 °C were 830 m^2 g^{-1} and 0.426 cm^3 g^{-1},

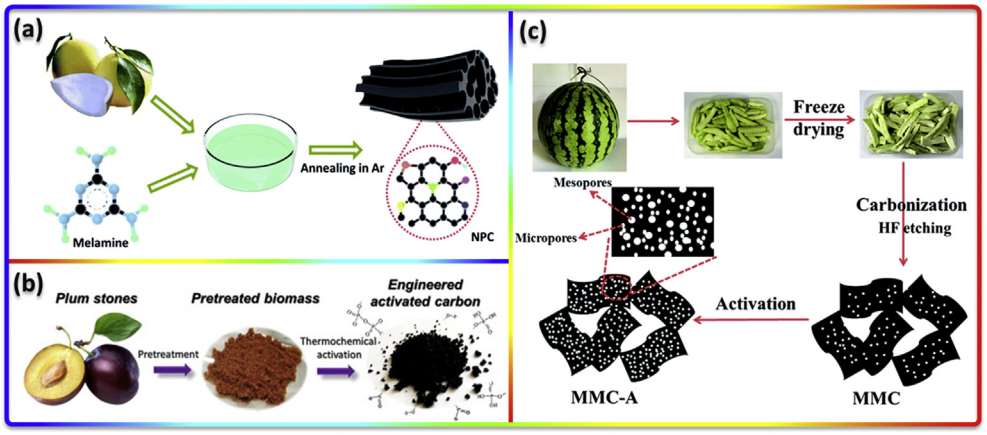

Fig. 5. (a) Formation of nitrogen-doped porous carbon. Adapted from the literature [152]. (b) Preparation of engineering ACs from plum stones. Adapted from the literature [153]. (c) Preparation of micro/mesoporous carbon (MMC) sheets heated at 800 °C for 3 h with a heating rate of 5 °C min^{-1}. Adapted from the literature [154].

respectively. Plum stones also can be used as a precursor for preparation of low-cost ACs, as shown in Fig. 5b. The surface area and pore volume of the porous ACs were 2174–3228 m^2 g^{-1} and 1.09–1.61 cm^3 g^{-1}, respectively, showing different acid-base characters of the surface. A suitable procedure of carbonization and activation can produce ACs with a high capacity of nitrogen dioxide [151]. In Fig. 5c, the watermelon peels were freeze dried, carbonized and then etched with HF to prepare a micro/mesoporous carbon (MMC). In the meantime, a $KHCO_3$ activation process was employed to obtain the MMC sheets. The $KHCO_3$ can decompose when heated and generate gases including CO_2 and CO, which can enlarge the size of a portion micropores and render them become mesopores. Moreover, the activator and gas can react with carbons, which contribute to the formation of another portion of mesopores and micropores. The specific surface area and pore volume of MMC sheets were 2360 m^2 g^{-1} and 1.31 cm^3 g^{-1}, respectively.

Similarly, Zhang, Xiang, Dong, Liu, Wu, Xu and Du [44] fabricated a 3D-structured highly porous AC foam with micro- and mesoporosity through carbonizing pomelo peel via KOH activation. The BET surface area of the AC foam was approximately 1533 m^2 g^{-1}. Liang et al. [155] also reported a 3D honeycomb-like porous carbon using pomelo peels as carbon precursors via KOH activation. The specific surface area of the obtained porous carbon was about 2725 m^2 g^{-1}, with numerous micropores (0.7–2.0 nm) and mesopores (2.0–3.3 nm). Furthermore, Molina-Sabio and Rodrıguez-Reinoso [54] found that olive and peach stones can be used as precursors for granular ACs with a highly developed microporosity and uniform micropores.

2.4.2. Tree-derived materials

Plants are a naturally abundant and renewable resource that can be converted into useful materials and energy, since they have a particularly rapid growth rate, short maturation cycle and high production yield [156]. For instance, bamboo, which belongs to the sub-family *Bambusoidae* of the family *Poaceae* (Graminae), is the most diverse group of plants in the grass family, and it takes only several months to reach full height. Approximately 1500 commercial applications of bamboo have been identified in the literature [157]. In China, India, Malaysia and other countries, bamboo has traditionally been used as a structural material to construct various living facilities and tools, since it is a strong, tough and low-cost material [158].

As shown in Fig. 6, Jiang et al. [92] proposed a strategy to convert disposable bamboo chopsticks into uniform carbon fibers by a controllable hydrothermal process performed in alkaline solutions. Similarly, Zhou, et al. [159] prepared a bamboo-based activated carbon with a BET surface area of ~700 m^2 g^{-1} and an average pore size of 3.3 nm via an activation process. In general, bamboo exhibits fairly constant compositions of lignin, cellulose and hemi-cellulose with a well-connected 3D microtexture [159]. The bamboo-derived carbon after carbonization has a hierarchical porous structure and a large surface area, which can provide high conductivity and highly-ordered microtexture. These properties facilitate ion transport by providing low-resistance pathways, thus offering the potential for application as supercapacitor electrodes electrodeposited into the bamboo carbon. Chen et al. [156] successfully synthesized a nitrogen and boron co-doped carbon with the hierarchical porous structure using bamboo via KOH activation. The obtained carbon material exhibited an excellent electrochemical activity and cycling stability, as well as a high specific capacitance and high energy density over other materials.

Deng et al. [22] reported a one-pot methodology for hierarchically porous carbons (HPCs) by mixing the carbon precursors and the leavening-reagents (e.g., $KHCO_3$), followed by undergoing an elevated temperature treatment, as shown in Fig. 7a. With the $KHCO_3$-assisted pyrolysis, the hydroxyl groups in cellulose and hemicellulose would undergo dehydration condensation among different parent polymers. Fig. 7b shows the SEM images with different mass ratios of cellulose, hemicellulose, and lignin. The results indicated that the derived HPCs exhibited a macroporous structure when containing less than 50% of lignin.

Elm is a tree widely spread throughout the northern hemisphere, especially in Northeast Asia. Fresh elm samaras are light-green oval flakes appearing in branches in spring, and they become pale-yellow and dry as plant wastes on the ground in summer. Typically, fresh elm samaras contain 85.0% water, 8.5% carbohydrates, 3.8% protein, 1.0% fat, and 1.3% dietary fiber. Chen, Yu, Zhao, Du, Tang, Sun, Sun, Besenbacher and Yu [66] fabricated porous carbon nanosheets (PCNS) from dry elm samara using a simple carbonization and activation treatment, as shown in Fig. 8a. Two strategies have been demonstrated for the achievement of a highly accessible surface area. One is to construct hierarchical porous structures combining micro-, meso- and macro-pores, while the other is to design 3D scaffolding frameworks of porous carbons that avoid overlapping-induced SSA loss and favor ion diffusion by providing short pathways. The PCNS products have an SSA of approximately 1990 m^2 g^{-1} and a high specific capacitance of 470 F g^{-1} (Fig. 8b).

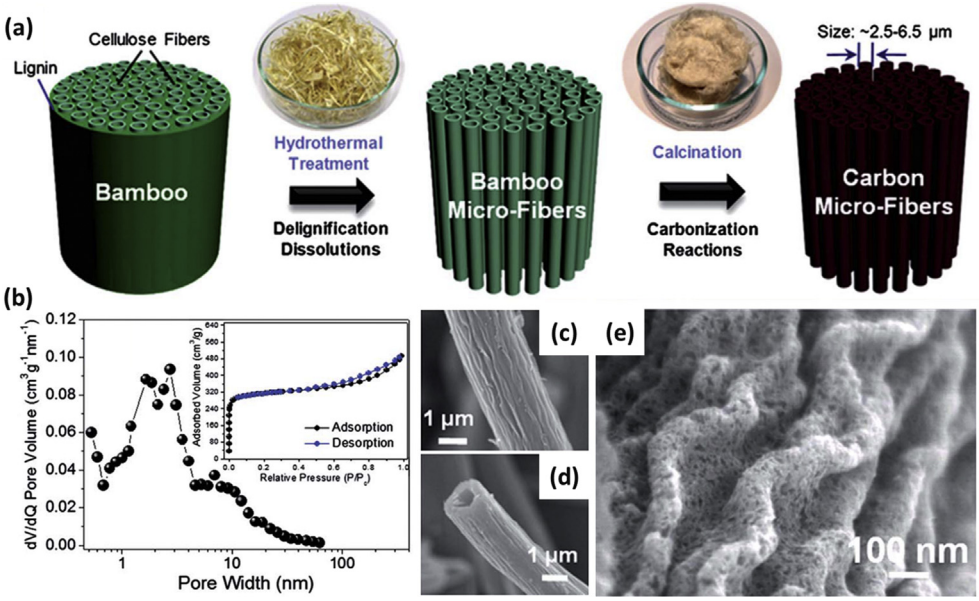

Fig. 6. Schematic diagram of (a) converting bamboo chopsticks into uniform carbon fibers. (b) pore-size distribution of produced carbon fibers. (c–d) optical images and (e) SEM images of uniform carbon fibers. Adapted from the literature [92].

2.4.3. Rice husk-derived materials

Agricultural byproducts and residuals, such as bagasse and rice husk, can be used as precursors for producing porous AC. Rice is the most widely consumed staple food in the world, especially in Asia. The estimated annual global production of 800 million tons of sugarcane results in 240 million tons of bagasse; similar, the annual world rice production is approximately 571 million tons resulting in ~140 million tons of rice husk annually [160]. Both bagasse and rice husk have been widely utilized in numerous applications, such as animal feeds, fuels for electricity and steam/heat generation, and raw materials for manufacturing paper and board. However, there is still a surplus of residues that pose a disposal issue for mill owners. Rice husk is the hard protective cover of the rice grain. After harvesting, the grain together with the husk undergoes further processing to remove the hull. Typically, the compositions of rice husk include cellulose (35–45%), hemicellulose (19–25%), and lignin (20%) [161].

Malik [162] prepared AC from sawdust and rice husks, which were utilized as adsorbents for the removal of acid dyes from aqueous solution. The sawdust and rice husks, collected from a local saw-mill and rice-mill, respectively, were separately carbonized in air. Similarly, Guo et al. [95] successfully prepared ACs with good adsorptive capacity from rice husks via KOH/NaOH activation at relatively low temperatures. The as-prepared rice husk was carbonized at 350–500 °C under a nitrogen atmosphere. The carbonized product was first activated by KOH or NaOH at 350–400 °C for up to 1 h to dehydrate the combination, and then the temperature was raised to 650–850 °C for 1 h to activate the combination. After that, the activated product was ground, washed with water and dried at 120 °C to form porous AC. Its specific surface area was high at about 3000 $m^2\ g^{-1}$ with a pore volume of 1.9 $cm^3\ g^{-1}$.

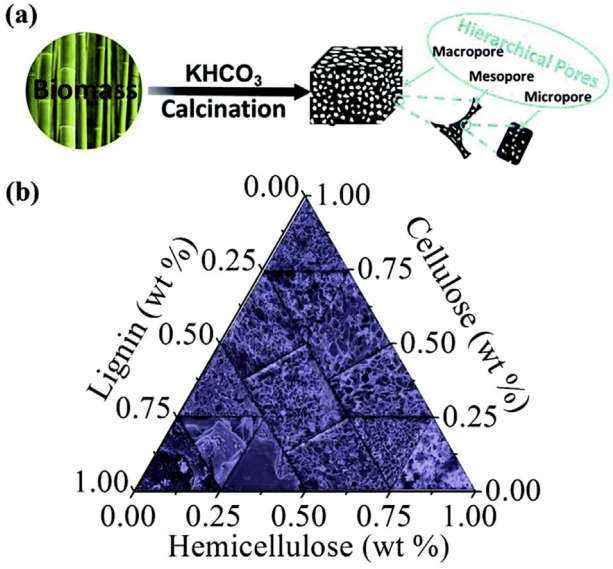

Fig. 7. (a) Formation of hierarchically porous carbons (HPCs) by mixing biomass with "leavening" agents followed by pyrolysis under an inert gas, and (b) SEM images with different mass ratios of cellulose, hemicellulose and lignin. Adapted from the literature [22].

2.4.4. Other precursors

In addition to the aforementioned materials, 2D and 3D carbon nanoarchitectures with excellent physico-chemical properties could be successfully derived from other plant-based materials, such as corn cobs, corn leaves and corn fibers. To enhance the specific surface area of the ACs, Moreno-Castilla et al. [163] reported that the byproduct of olive mills could be used as raw materials to produce AC via chemical activation or physical activation. The obtained results indicated that chemical activation at 800 °C yielded ACs with high specific surface area in an inert atmosphere.

3. Applications of plant-derived materials for energy storage devices

Recently, carbon materials derived from biomass has become particularly attractive and sustainable in the field of energy storage. In particular, high-performance ACs based on inexpensive and abundant biomass are highly preferred. Biomass-based nanomaterials used as electrodes for energy storage devices exhibit

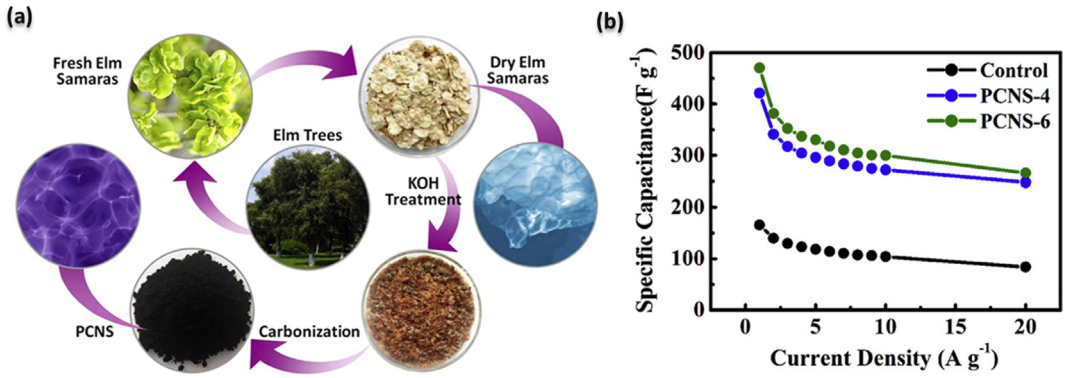

Fig. 8. (a) Schematic illustration of porous carbon nanosheets (PCNS) derived from dry elm samaras. (b) Gravimetric capacitances at different current densities. Adapted from the literature [66].

relatively high performance due to their high conductivity and accessible SSA. Other review articles have demonstrated the benefit of using a biomass/bionic approach, i.e., energy-efficient, green, low-cost and possibly large-scale synthesis for carbon materials [164,165]. In this part, the performance of plant-based biomass electrodes for EES applications, including LIBs, LiSBs, sodium ion batteries (SIBs) and supercapacitors, are reviewed and illustrated.

3.1. Lithium ion batteries (LIBs)

LIBs are a type of rechargeable battery where lithium ions move from the anode (negative electrode) to the cathode (positive electrode) during discharge and back when charging. Graphite has been widely used as anode materials in LIBs; however, commercial graphite typically suffers from low energy density (i.e., a theoretical capacity of 372 mAh g^{-1}). Thanks to various biotemplate synthesis techniques, as–fabricated carbon materials with various textures, morphologies and crystallinities have received considerable attention as anodes. Extensive studies on developing plant-based biomass anode materials in LIBs, such as egg white-derived protein [166], cherry stones [167], green tea leaves [128], banana peels [168], and hazelnut shells [169], have been carried out.

Plant-derived biomass materials usually exhibit intriguing structures, such as hierarchical organization, periodic patterns and special nanoarchitectures. These structures can confer certain unique functionalities, including anti-reflection, superhydrophobicity, structural coloration and biological self-assembly [170]. For instance, Li et al. [166] obtained a hierarchically mesoporous and partially graphitized carbon with an SSA of ~806 m^2 g^{-1} and a bulk N content of 10.1% by templating the structure of cellular foam with proteins derived from egg white. The corresponding lithium storage capacity was approximately 1780 mAh g^{-1}. It was demonstrated that plant-derived proteins could serve as an ideal precursor for synthesizing carbon materials. Similarly, Xing, et al. [171] demonstrated a high capacity for lithium intercalation by pyrolyzing sugar, where a reversible capacity of 650 mAh g^{-1} was obtained. Furthermore, Arrebola, et al. [167] found that cherry stones show promise as the anode material in LIBs, yielding ACs with a specific capacity of 200 mAh g^{-1} at 5 C.

Han et al. [128] pyrolyzed the carbonaceous materials from green tea leaves for applications as anodes in LIBs, as shown in Fig. 9a. The results indicated that carbon pyrolyzed at a relatively low temperature of 700 °C would contain numerous functional groups. The samples exhibited a relatively high capacity of 471 mAh g^{-1} at the 50th cycle (Fig. 9b and c). Moreover, carbon specimens pyrolyzed at 700 °C displayed an excellent high-rate capability of 131 mAh g^{-1} at 10 C. Similarly, banana fibers treated with pore-forming substances, such as $ZnCl_2$ and KOH, were promising candidates as the anode materials in LIBs. Stephan, Kumar, Ramesh, Thomas, Jeong and Nahm [168] synthesized the disordered carbonaceous materials from banana fibers. The product obtained with $ZnCl_2$ treatment yielded first-cycle lithium insertion and deinsertion capacities of 3325 and 400 mAh g^{-1}, respectively.

Hazelnut shells have been extensively used for applications ranging from ingredients in fireplace logs to creative landscaping because they do not decompose readily at high temperatures. For example, Unur et al. [169] have successfully introduced porosity to hydrochar (HC) via solar heat treatment, KOH activation and MgO templating. The obtained microporous materials were tested as Li–ion intercalation hosts in LIBs using 1 M $LiPF_6$ in EC/DMC as an electrolyte. Their capacities at a rate of 1C were stable reversible and comparable to the maximum theoretical capacity of graphite. In particular, the MgO–templating HC (an SSA of 150 m^2 g^{-1}) exhibited the best LIB cycling performance, i.e., 307 mAh g^{-1} at the 100th cycle under room temperature. Similarly, Yi, et al. [172] fabricated graphene/Fe_3O_4 nanocomposite (GCS/FO-NC) from the soda paper-making black liquor, as shown in Fig. 10a. The initial discharge specific capacity and reversible capacity after 1400 discharge/charge cycles of the GCS/FO-NC were 1385 mAh g^{-1} and 750 mAh g^{-1}, respectively, as shown in Fig. 10b. In addition, the Coulomb efficiency was close to 100% after 3 cycles and could be maintained indefinitely.

Extensive efforts have been devoted to developing sustainable and high-performance electrode materials from plant-derived biomass for LIBs. The above review suggests that biomass-derived carbons can offer a higher capacity than commercialized graphite, since biomass intrinsically has desirable molecular structures and architectures, which are favorable for charge storage and transport.

3.2. Lithium-sulfur batteries (LiSBs)

Biomass-based porous carbon could act as an effective electronic conductor to enhance the use of active materials in LiSBs (Fig. 11). Carbon materials used for LiSBs require a high contact area between electrode and electrolyte. The practical energy density of the packaged LiSBs can reach 400–600 Wh kg^{-1}, which could enable a traveling distance of 500 km for EVs. However, commercial LIBs still cannot realize the insulating nature of sulfur and its active mass shuttling loss. In addition, long chain polysulfides dissolve into the electrolyte and migrate to the lithium anode, which causes the polysulfide shuttle effect. The ultimate goal of material design and development is to achieve the best large-scale performance with proper structure and composition modification. Therefore, in

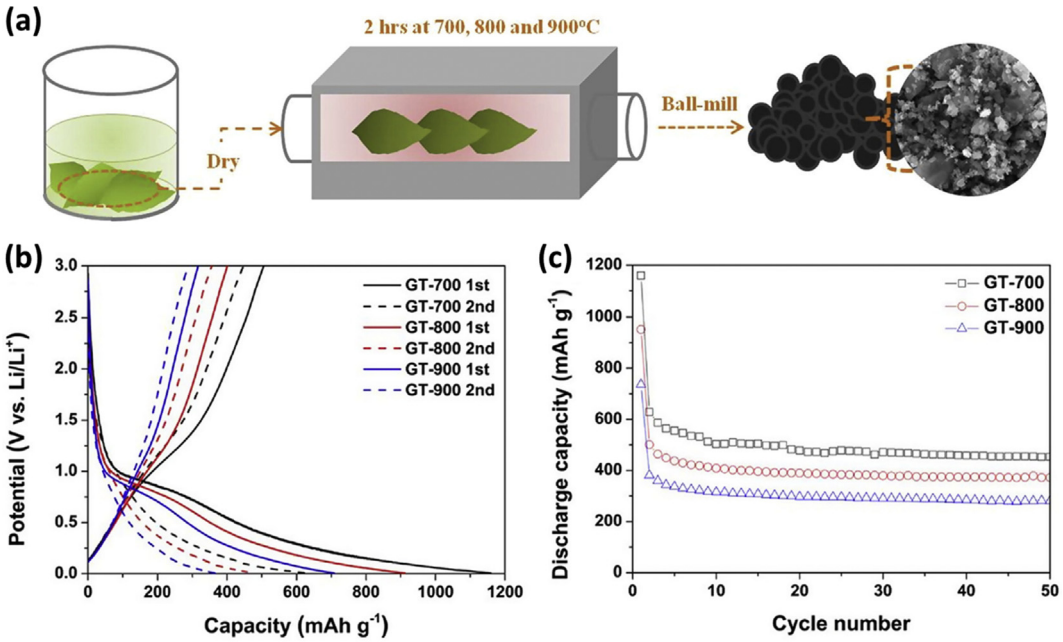

Fig. 9. (a) Synthesis procedure for pyrolytic carbons from green tea; (b) 1st and 2nd charge–discharge profiles of electrodes pyrolyzed at 700 °C (GT–700), 800 °C (GT–800), and 900 °C (GT–900); and (c) cell performance curves at specific current densities (0.1 C = 37.2 mA g^{-1}). Adapted from the literature [128].

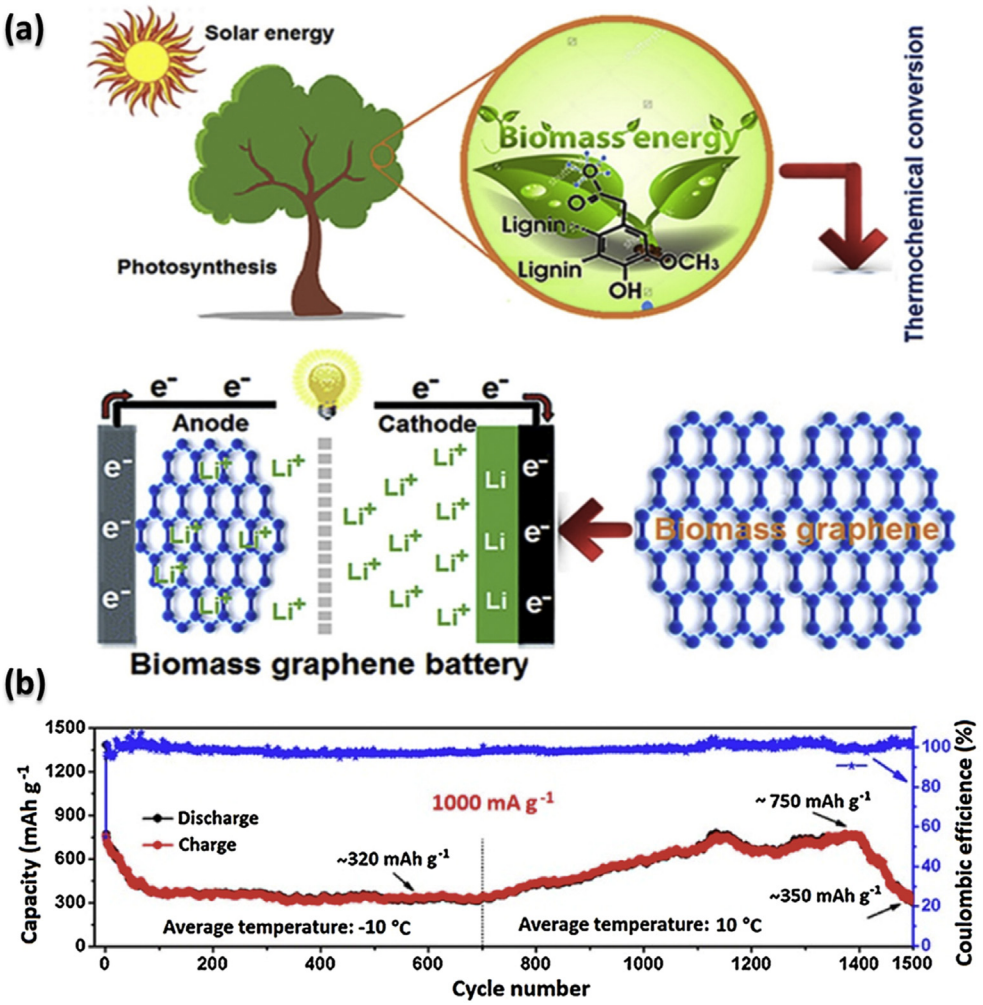

Fig. 10. (a) Graphene-like carbon sheet prepared from soda paper-making black liquor, and (b) Cycling stability of the GCS/FO–NC–D electrode at a high current density of 1000 mA g^{-1} for LIBs. Adapted from the literature [172].

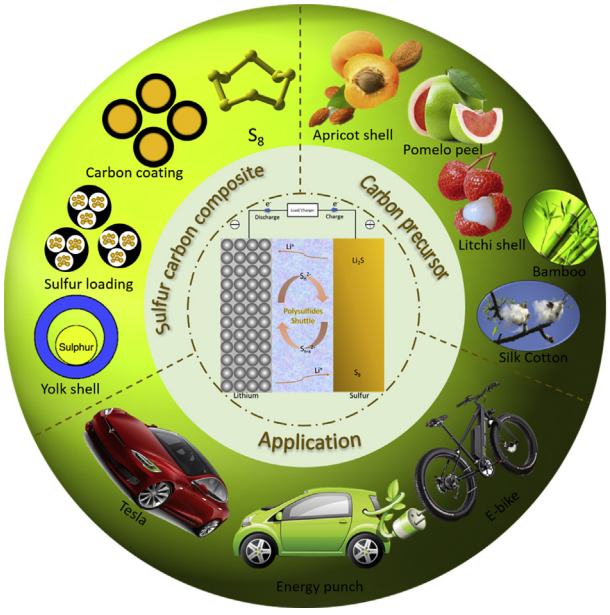

Fig. 11. Sulfur carbon composite from biomass precursors for LiSBs in various applications.

this part, plant-derived materials, such as coconut shells, bamboo and rice husks, are reviewed and discussed.

Extensive efforts have been dedicated to developing high-performance electrode materials from plant-derived biomass for ultrahigh capacity LiSBs. Table 2 presents the performance of plant-derived porous carbon materials used in LiSB applications. For instance, Zhang's group [44] has been dedicated to developing carbon materials from pomelo peel for rechargeable LiSBs. The obtained nanocomposite with 60 wt% sulfur showed an initial discharge capacity of ~1260 mAh g^{-1} at a rate of 0.2 C and retained a specific capacity of 750 mAh g^{-1} with 96% coulombic efficiency after 100 cycles. Olive stone could be used as an alternative to petrol or diesel, Moreno, et al. [173] obtained AC from olive stones to fabricate a sulfur/carbon composite for cathode of LiSB. The as-prepared electrode with 80 wt% sulfur loading delivered a specific capacity of 670 mAh g^{-1}. Guo et al. [174] also successfully obtained PCNS with a high SSA using corncob residuals as carbon precursors. The S/PCNS composite exhibits an initial discharge capacity of 1600 mAh g^{-1} and maintains a reversible capacity of 554 mAh g^{-1} after 50 cycles. The excellent performance may be attributed to the high porosity and 2D structure of carbon nanosheets. The obtained structure not only provides a stable and continuous pathway for rapid electron and ion transport but also restrains soluble polysulfides and suppresses the shuttle effect. In addition, the large SSA and unique 2D (sheet-like) structure of PCNS results in a high utilization of sulfur, which is suitable for serving as cathode materials in LiSBs.

ACs by pyrolysis of natural waste apricot shell were fabricated by Yang et al. [175]. The sample with a BET surface area of ~2270 m^2 g^{-1} and a pore volume of 1.05 cm^3 g^{-1} was able to effectively hold the sulfur and restrain the diffusion of polysulfides during the charge-discharge cycle for a rechargeable LiSBs. The initial discharge capacity of 1277 mAh g^{-1} can be obtained at 0.1 C. After 200 charge-discharge cycles, the discharge capacities at a current density of 0.2 C and 1 C were about 710 and 613 mAh g^{-1}, respectively. Similarly, AC with a specific surface area (i.e., ~3160 m^2 g^{-1}) and large pore volume (i.e., 1.88 cm^3 g^{-1}) was prepared from waste litchi shells with channel-like macropores by Zhang et al. [176]. At a current density of 200 mA g^{-1}, the initial discharge capacity of the resulting AC/S composite cathode with a sulfur content of 60% is about 1100 mAh g^{-1}. At a current density of 800 mA g^{-1}, it exhibits 51% capacity retention over 800 cycles with a fade rate of 0.06% per cycle, and the Coulombic efficiency remains at ~95%.

Ye et al. [177] reported the preparation of uniform carbon precursor spheres with diameters of 300 nm via a hydrothermal process of D-glucose. The carbon precursor was involved in KOH activation followed by an annealing process to obtain microporous/mesoporous carbon spheres (MPCSs). Sulfur was introduced into MPCSs to obtain the S–MPCS composite. The as-prepared composite showed a high specific capacity, favorable rate capabilities and a long cycle life of 800 cycles at 1 C. This may be attributed to the advanced porous carbon spheres with a large proportion of micropores and moderate activation. Zhou, et al. [178] fabricated a natural polymer, amylopectin wrapped GO-S nanocomposite. It was found that the branched amylopectin wrapped GO–S could confine the sulfur particles among the GO layers, which helps to restrain the diffusion of polysulfides during the discharge-charge cycles. The GO–S–Amy electrodes exhibited initial capacities of approximately 820, 650 and 600 mAh g^{-1} under rates of C/8, 5C/16 and C/2, respectively.

Attracted by the unique tissue and functions of leaves, Chung and Manthiram [179] prepared a natural carbonized leaf (CL) as a polysulfide diffusion inhibitor in LiSB. The CLs are carbonized without any time-consuming, hard template, or multistep treatments. The free-standing CL thin films have an anatomically hierarchical microstructure, which could intercept the migrating polysulfides (Fig. 12a). Also, the CL has an integral carbon framework (for transporting electrons), an abundant micro-/mesoporous structure (for storing the trapped active material), and an intrinsic macroporous network (for absorbing the electrolyte), as shown in

Table 2
Comparison of plant-derived porous carbon materials used in LiSB applications.

Carbon precursor	S_{BET} (m^2 g^{-1})	Sulfur content (wt.%)	Discharge capacity (mAh g^{-1})		Capacity retention (%)	Cycle life (times)	Rate (C)	Reference
			Initial	Final				
AC (commercial)	1200	54	1370	850	62.0	50	0.2	[180]
Banana	2741	65	1200	570	47.5	500	1	[40]
Pomelo peel	1533	60	1258	750	59.6	100	0.2	[44]
Corncob	1198	68	1600	634	39.6	50	0.1	[174]
Apricot shell	2269	54	1193	733	61.4	200	0.2	[175]
Litchi shell	3164	60	1105	800	72.4	100	0.5	[176]
Olive stone	587	70	800	670	83.8	100	0.05	[173]
Glucose	1194	50	1420	750	52.8	100	0.1	[177]
Bamboo	792	50	1262	550	43.6	150	–	[125]
Silk cocoon	3243	48	1443	804	55.7	80	0.5	[181]
Soybean residue	2690	64.5	699	436	62.4	600	1	[182]
Seedpod shell	2923	86.5	1138	1116	98.1	100	0.5	[93]

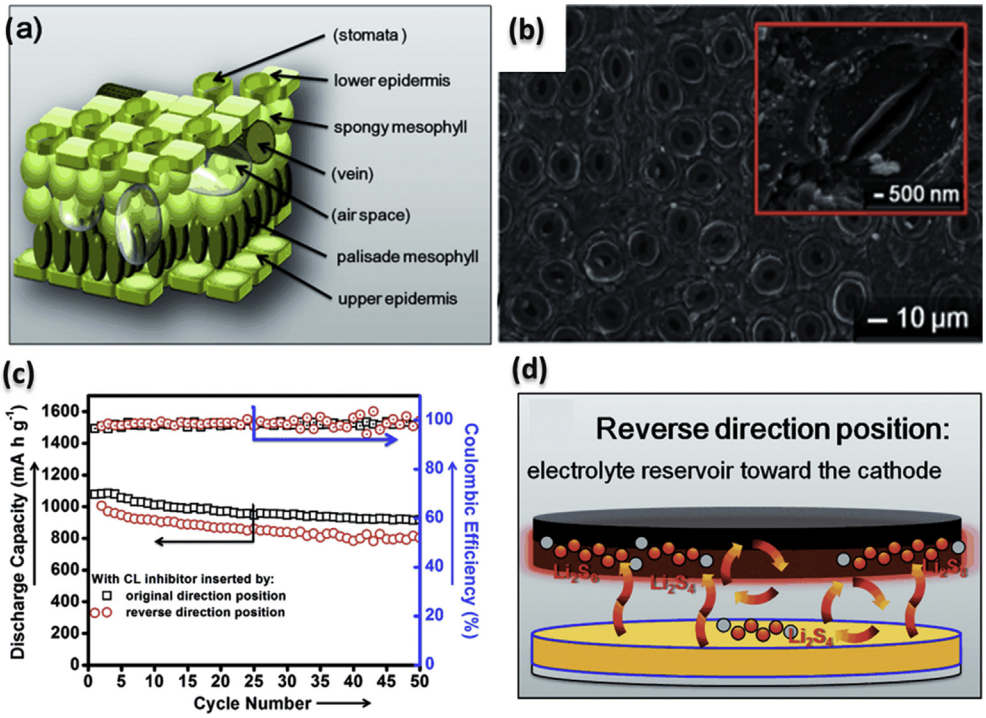

Fig. 12. (a) Schematics of the leaf, (b) Cyclability of the cells with the CL inhibitor inserted with two opposite direction positions at a C/5 rate, (c) surface of the electrolyte reservoir, and (d) reverse direction position. Adapted from the literature [179].

Fig. 12b. LiSB with the CL polysulfide diffusion inhibitors exhibits a high discharge capacity (1320 mA h g^{-1}), high Coulombic efficiency (98%), and superior cycle stability over 150 cycles (Fig. 12c and d).

3.3. Sodium ion batteries (SIBs)

Recently, SIBs have attracted great interests as a low-cost alternative to LIBs due to the widespread distribution of sodium. However, sodium ion has a larger ionic radius than that of lithium ion. Therefore, the challenge for SIBs development is to design suitable host materials with a larger space for intercalating and accommodating sodium ions [94]. Fig. 13a illustrates the material synthesis process of hierarchical porous carbons (HPCs), and its relevant charge storage mechanisms. Charge storage in carbon anodes can be broken down into four major mechanisms: (1) physisorption on the surface of pores, (2) chemisorption on surface heteroatoms or at defect sites, (3) intercalation between graphene layers, and (4) filling within metal pores. In general, sodium ions can be stored in randomly stacked graphene layers and/or micropores. As shown in Fig. 13c, the HPC electrodes exhibit excellent rate capability (i.e., 148–226 mAh g^{-1} at a current density of 0.1 A g^{-1}), which might be attributed to the combination of interconnected sheet-like structure, large interlayer space and highly developed porosity. The HPCs prepared without a hydrothermal process (Route 2) shows better cycling performance than that of the electrodes prepared with a hydrothermal/KOH mixing process (Route 1), as shown in Fig. 13d. Similarly, H_3PO_4 activation can be introduced to the functional groups on the surface of carbon for obtaining electrodes with a well-developed porous structure for SIBs [183].

Wang et al. [94] derived hierarchical porous carbons as an anode of SIBs using peanut skin. It estimates that over 30 million tons of peanut were produced annually around the world. Peanut skin contains about 12% protein, 16% fat, and 72% carbohydrate. The SSA of the hierarchical porous carbon is about 1400 m^2 g^{-1}. Peanut skin derived carbon exhibits initial charge capacity of 431 mAh g^{-1} at 0.1 A g^{-1}, retaining a reversible capacity of 47 mAh g^{-1} at 10 A g^{-1}, and showing a capacity retention of 83–86% after 200 cycles. Similarly, sucrose is an abundant carbon precursor for producing hard carbon. Li et al. [184] fabricated monodispersed hard carbon spherules coated with soft carbon, indicating that the coating can significantly improve the initial Coulombic efficiency to 83%. The $Na_{2/3}Ni_{1/3}Mn_{2/3}O_2$/HCS1600 cell is capable to provide a high operating voltage (i.e., 3.5 V), a high capacity (>300 mAh g^{-1} based on the negative electrode) and a high initial Coulombic efficiency (i.e., 76%).

It is noted that N and O functionalization can improve the electrochemical performance of carbon-based sodium anodes due to enhanced reactivity and electronic conductivity [143,185]. Xu et al. [72] synthesized broad beans-derived porous carbon materials with heteroatom doping (Fig. 14a). The SSA and total pore volume of the as-prepared materials are in the range of 10–655 m^2 g^{-1} and 0.01–0.38 cm^3 g^{-1}, respectively. Four major nitrogen peaks for the porous carbon material derived from broad beans can be found (Fig. 14b): (1) N-oxides of pyridine-N (N1) at 403.3 eV, (2) quaternary-N (N2) at 401.0 eV, which is the most stable nitrogen species in the carbonization process, (3) pyrrolic-N (N3) at 399.9 eV, and (4) hexagonal pyridinic-N (N4) at 398.5 eV. When the as-prepared electrode was employed as the anode in SIBs, the initial discharge capacity is about 466 mAh g^{-1} at a current density of 200 mA g^{-1}.

3.4. Supercapacitors

Supercapacitors and batteries are the most effective electrochemical energy conversion and storage devices for practical application [170]. Supercapacitors lying between electrochemical batteries and conventional capacitors are promising energy storage devices due to their excellent power density and low maintenance cost. Electrode materials play an important role in the development

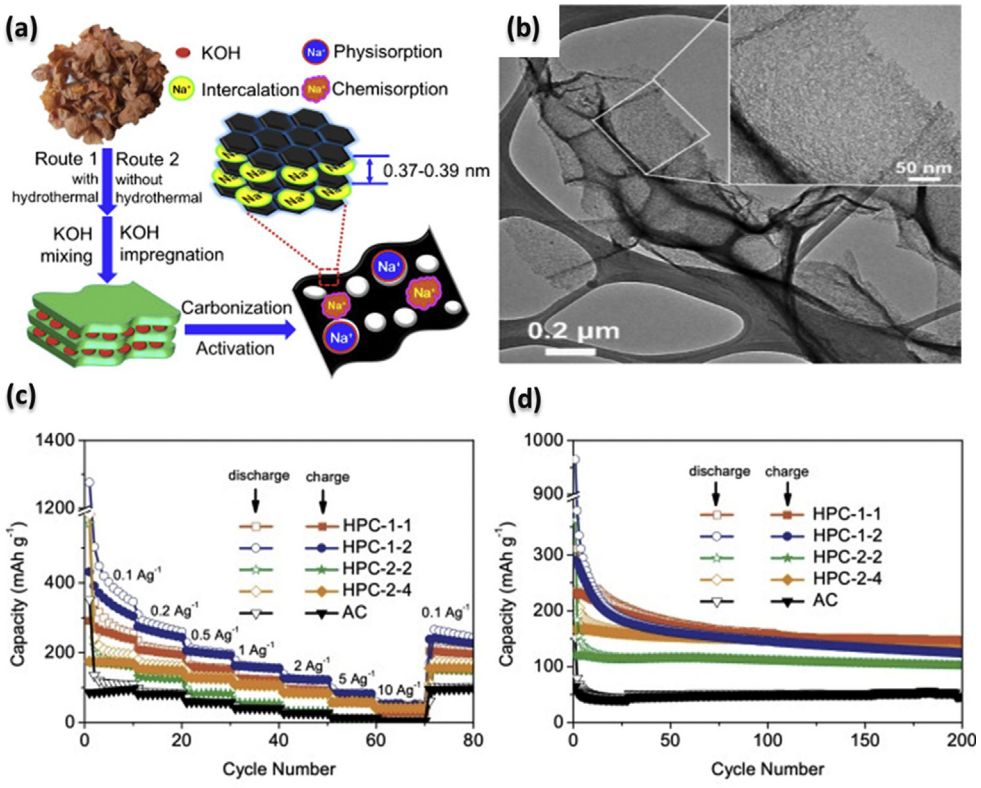

Fig. 13. (a) Formation of hierarchical porous carbons (HPCs) and its relevant charge storage mechanism; (b) TEM image; (c) Rate performance of HPCs and commercial AC; and (d) Cycling capacity retention of HPCs and AC. Adapted from the literature [94].

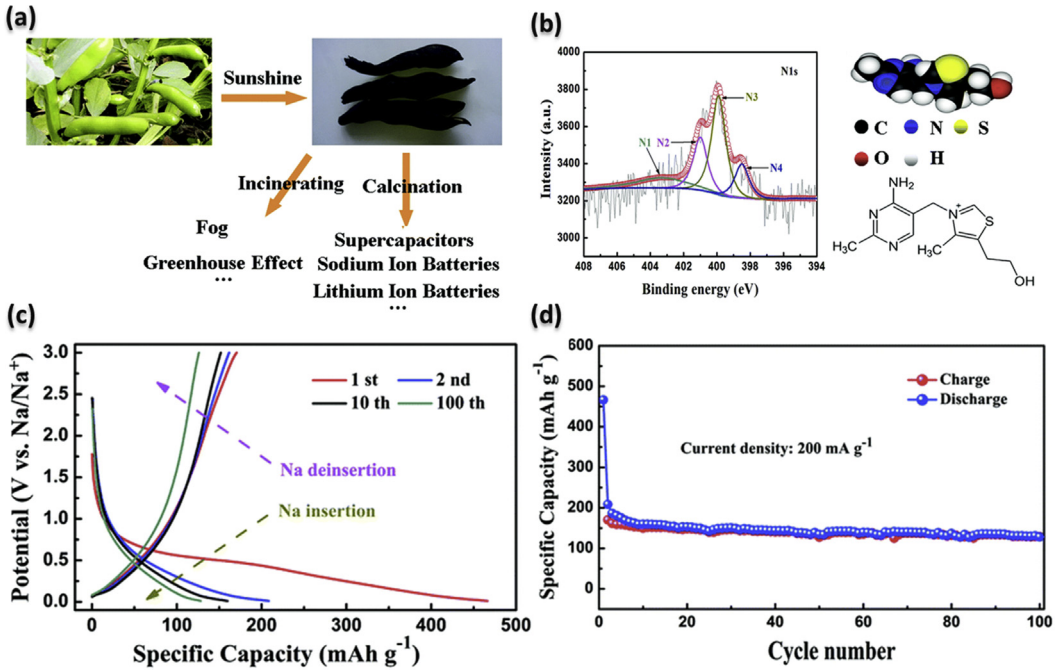

Fig. 14. (a) Different processing methods of SIBs. (b) XPS spectra for porous carbon material from broad beans: N1 (N-oxides of pyridine-N); N2 (quaternary-N); N3 (pyrrolic-N); and N4: (pyridinic-N). (c) Galvanostatic charge/discharge profiles, and (d) cycling performance of the bean-derived anode for SIBs at a current density of 200 mA g^{-1}. Adapted from the literature [72].

of high-performance supercapacitors to meet the requirements of advanced electronics and energy systems. It is noted that plant-based biomass, such as bamboo [156], watermelon [186], peanut shells [187], rice husks [98], cattails [188], argan seed shells [90], cornstalks [189], and sunflower seed shells [130], are suitably used as a precursor for fabricating porous carbon. In this part, the performance of plant-derived biomass carbon materials in supercapacitors is illustrated.

Nature provides unlimited sources for the fabrication of novel artificial materials with special structures and properties. Table 3 presents the physico-chemical characteristics of AC synthesized for supercapacitors in the literature. Rice, rich in carbon and nitrogen contents, is the most widely consumed staple food around the world. With the use of fermented rice, Gao et al. [96] prepared N-doped carbon spheres with a high SSA (e.g., 2105.9 $m^2 g^{-1}$) and a high porosity (e.g., 1.14 $cm^3 g^{-1}$). Supercapacitors with the fabricated porous N-doped carbon spheres exhibited a great capacitance of 219 F g^{-1} at a current density of 15 A g^{-1}, as well as excellent stability for over 4400 cycles.

Mesopores on carbon materials may accelerate ion transport rate, thereby achieving a better capacity for supercapacitors. Auricularia are cultivated more than 460,000 tons per year around the world. Inspired by the inherent meso/macroporous architecture of auricularia, Zhu, et al. [190] synthesized 3D graphene incorporated hierarchical porous carbon (GHPC) nanohybrids, as shown in Fig. 15a. The GHPC nanohybrids exhibited a specific surface area of up to 1723 $m^2 g^{-1}$, with a mesoporosity of ~75% and a pore volume of 1.85 $cm^3 g^{-1}$. The developed structure can not only provide better ion transport pathways because of the introduction of mesopores, but also accelerate electron transport rate due to incorporated graphene into 3D porous carbon. Therefore, a high specific capacitance of 256 F g^{-1} at 1 A g^{-1} can be achieved with a long cycle life (92% retention after 10,000 cycles) in 1 M H_2SO_4 for symmetric supercapacitors, as shown in Fig. 15e.

Chen et al. [156] prepared bamboo-derived porous carbon with B and N co-doping as an electrode material in supercapacitors. The supercapacitors with electrodes based on the as-obtained materials exhibited high specific capacitance, i.e., 281 and 318 F g^{-1} in KOH (1 M) and H_2SO_4 (1 M), respectively. The results were attributed to the high electrochemical activity enhanced by the hierarchical porous structure, as well as by B and N co-doping. Similar observation for biomass-derived carbon materials with S and N co-doping can be found elsewhere in the literature [72].

Cattails, wetland plants with a unique flowering spike, burst under dry conditions. As observed by SEM, well-developed porous carbon foam with macropore sizes of 1–2 μm is clearly observed for a one-step synthesis. Fan, Qi, Xiao, Yan and Wei [188] has indicated that the one-step synthesis of biomass-derived porous carbon foam could yield specific capacitance values of 336 F g^{-1} as the scan rates range from 2 to 500 mV s^{-1}. Similarly, watermelon can be employed as carbonaceous gel-based materials. In Xu's group [186], materials fabricated from watermelon exhibited a high capacitance of 333 F g^{-1} at a current density of 1 A g^{-1} within a voltage between −1 and 0 V. These materials also showed outstanding cycling stability with 96% capacitance retention after 1000 cycles.

It is noted that extensive efforts have been dedicated to the development of high-performance electrode materials from plant-derived biomass for high power density supercapacitors [191]. The specific surface area, pore size distribution and final electrochemical performance of the obtained carbon materials depend on their biomass precursors and the activation methods used. According to the above review, it was found that supercapacitors with plant-derived biomass AC exhibited great capacitance with values generally three times higher than those of conventional AC electrodes.

4. Life cycle assessment for reclaimed batteries

4.1. Importance and significance of reclaimed battery

Resource depletion is an important consideration in sustainable development and waste management. Metal elements and poisonous substances in spent LIBs pose harmful impacts to human health and the ecosystem if batteries are arbitrarily discarded or improperly buried. Since batteries are among the costliest components of electric and hybrid vehicles [193], spent LIBs contain valuable materials that would provide some economic incentive for recycling. Moreover, lithium is geographically limited and politically sensitive. Spent batteries thus are increasingly being considered a potential resource for manufacturing new batteries. Although recycling processes have their own environmental impacts, these are generally less than those from primary production [194,195]. Also, manufacturing through the use of recycled electrode materials is less energy- and resource-intensive than the use of virgin materials, which can avoid significant environmental impacts, especially sulfur oxides (SO_x) emissions and water contamination [196,197]. A similar study revealed that recycling and reuse of metal components from spent LIBs via an integrated recycling process could lower the ecological impacts by up to 49% [198]. These would serve as key motivators for spent battery recycling regardless of the energy intensity of assembly. Furthermore, recycling of materials can avoid additional processing costs for waste treatment. However, only 3% of waste LIBs have been recycled, corresponding to a ratio of total lithium recycling less than 1% [199].

Table 3
Physico-chemical characteristics of activated carbons synthesized for supercapacitor applications.

Biomass	Activation method	S_{BET} ($m^2 g^{-1}$)	Specific capacitance (F g^{-1})	GCD measurement[a]	Electrolyte	Reference
Coffee endocarp	Physical activation	709	176	1 mA cm^{-1}	1 M H_2SO_4	[192]
Oil palm	Physical activation	1704	150	10 mA cm^{-2}	–	[75]
Sunflower seed shell	KOH activation	2509	311	250 mA g^{-1}	30 wt% KOH	[73]
Corn grain	KOH activation	3199	257	1 mA cm^{-2}	6 M KOH	[82]
Spruce	KOH activation	2670	245	–	0.1 M NaOH	[83]
Lotus seedpod	KOH activation	1813	402	500 mA g^{-1}	6 M KOH	[84]
Mushroom (Shiitake)	KOH activation	2988	306	1000 mA g^{-1}	6 M KOH	[70]
Rice husk	KOH activation	2783	179	6250 mA g^{-1}	6 M KOH	[85]
Wheat bran	KOH activation	2189	294	500 mA g^{-1}	6 M KOH	[86]
Tea leaf	KOH activation	2841	330	1000 mA g^{-1}	2 M KOH	[87]
Pomelo peel	KOH activation	2105	44	500 mA g^{-1}	1 M $NaNO_3$	[88]
Bamboo	KOH activation	1251	260	1 mA cm^{-1}	30 wt% H_2SO_4	[89]
Cherry stone	KOH activation	1171	232	1 mA cm^{-2}	2 M H_2SO_4	[76]
Argan seed shell	KOH activation	2062	355	125 mA g^{-1}	1 M H_2SO_4	[90]
Fermented rice	$ZnCl_2$ activation	2106	219	15000 mA g^{-1}	0.1 M KOH	[96]
Rice husk	$ZnCl_2$ activation	1442	243	50 mA g^{-1}	6 M KOH	[97]
Peanut shell	$ZnCl_2$ activation	1634	245	50 mA g^{-1}	6 M KOH	[98]
Coffee bean	$ZnCl_2$ activation	1019	368	50 mA g^{-1}	1 M H_2SO_4	[99]

[a] GCD: Galvanostatic charge–discharge.

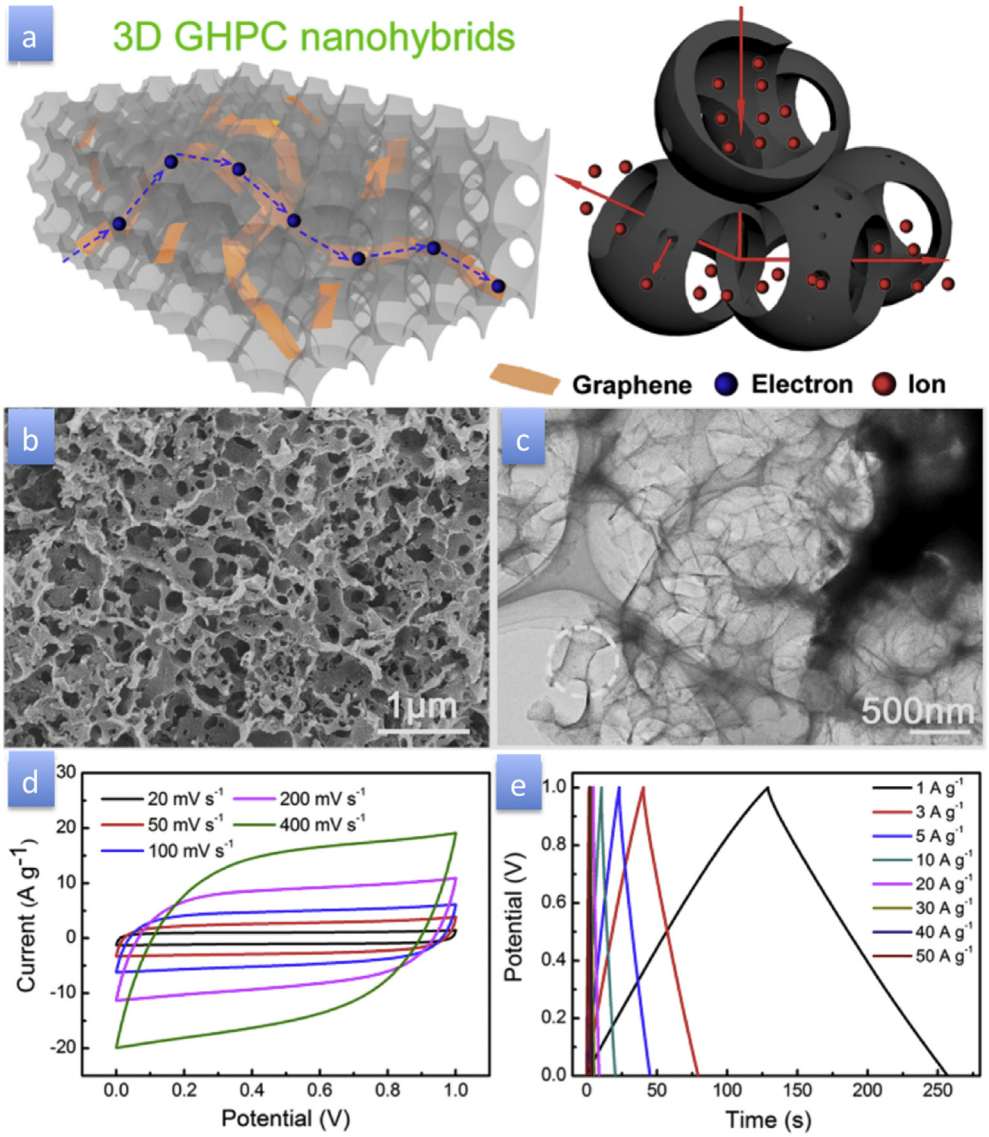

Fig. 15. (a) Schematic illustration, (b) SEM image, and (c) low-magnification of graphene incorporated hierarchical porous carbon (GHPC) nanohybrids for enhancing supercapacitor performance. Electrochemical performances evaluated by symmetrical two-electrode supercapacitors in 1 M H_2SO_4 aqueous solution: (d) CV curves of the GHPC at various scan rates, and (e) galvanostatic charge/discharge curves of the GHPC under different current densities. Adapted from the literature [190].

A typical battery cell consists of several key components including anode, cathode, electrolyte, separator, and current collectors. However, recycling of lithium-based batteries such as LIBs and LiSBs is more complicated than that of lead acid or nickel-metal-hydride batteries because lithium-based batteries have a wider variety of materials (i.e., greater chemical complexity) in a single cell. These various materials in LIBs, such as active powder components and metal foil, must be separated from each other during recycling [200]. Therefore, recycling of spent lithium-based batteries is generally a combination of unit processes that may include (i) discharging and dismantling, (ii) mechanical separation such as hammer-mill, (iii) filtering, (iv) supercritical fluid extraction, (v) a pyrometallurgical (smelting) process, and (vi) a hydrometallurgical process. 0 shows the generalized process flow sheet for recovery of lithium ions from leaching liquor. Leaching and precipitation play key roles in the entire recycling process [201]. In any case, separated streams for material processing are favorable to ensure the purity and quality of products for subsequent reuses.

Different recycling approaches offer different yields of components depending on the electrode materials and recycling routes. For instance, the supercritical CO_2 fluid can be applied to extract the electrolyte such as ethyl methyl carbonate, diethyl carbonate, and $LiPF_6$ from the cells [202]. In contrast, in a typical pyrometallurgical process, LIBs after having been dismantled to the module level will be introduced to a high-temperature shaft furnace, along with slag-forming agents such as limestone and sand. The electrolyte and plastics are burned to supply energy for smelting, while valuable metals such as copper, cobalt, nickel, and iron are reduced to an alloy, from which these valuable metals can be further recovered via leaching. However, the remaining elements including lithium, aluminum, silicon, calcium, iron, and manganese become the slag. Currently, recycling of aluminum or lithium from the slag is neither economical nor energy efficient [200]. Similarly, the hydrometallurgical process typically involves acid-base leaching, solvent extraction, chemical precipitation and electrochemical processes.

The cathode material for LIBs prevalent in consumer electronics is lithium cobalt oxide ($LiCoO_2$). Various combinations of Ni, Mn,

and Al can be used to replace the cobalt at different ratios, thereby increasing performance and lowering raw material cost. Since 2011, $Li–Ni_xCo_yMn_zO_2$ has been widely used in place of $LiCoO_2$ as an active material for the cathodes in LIBs [203]. Another promising low-cost cathode material is $LiFePO_4$. At present, industrial full-scale technologies for recycling iron, aluminum and copper metals from spent LIBs are available [204–206]. Recent developments in recycling have been focused on the recovery of cobalt and nickel due to their high price [203]. Only a few recycling routes are focused on lithium and manganese recovery [207]. Phosphate and graphite are normally not recycled in current industrial processes [208]. In any case, the recycled products must be of high enough quality to find a market for their original purpose; otherwise, an alternative market needs to be identified. Recently, Gao, et al. [209] demonstrated that formic acid can be used as both a leaching and separation reagent for metal recovery from cathode scrap. The overall recovery ratios of Al, Li, Ni, Co, and Mn were found to be 95.46%, 98.22%, 99.96%, 99.96%, and 99.95%, respectively. Similarly, Li and Co recoveries of nearly 100% and >90% could be achieved using citric or malic acids as leaching agents [197].

Recycling can recover valuable materials to achieve the required material quality at different stages of production, from basic building blocks to battery-grade materials. Researchers at the Argonne National Laboratory have been examining material demand and recycling issues related to LIBs [210], including (1) identification of the greenest and most economical recycling processes; (2) evaluation of the performance of current recycling practices or other advanced methods; and (3) quantification of the environmental impacts of battery production and recycling through Argonne's GREET (Greenhouse gases, Regulated Emissions and Energy use in Transportation) model. The GREET model has been continuously expanded to include new cathode and anode materials that can be used in quantifying the environmental impacts of EVs [211]. For life cycle assessment (LCA), a zero burden approach is typically used when assessing waste management (e.g., recycling) technologies since waste LCAs are conducted from a "gate-to-grave" approach [212].

4.2. Environment benefits and impacts

The increasing applications of rechargeable batteries in mobile and stationary energy storage have triggered a great interest in the environmental benefits and impacts associated with their life cycle [213]. LCA can be applied to estimate the performance and its associated potential environmental impacts and benefits of battery products over their lifetimes [214]. As shown in Fig. 16, LCA takes into account the entire life cycle from cradle (e.g., raw material extraction) to grave (e.g., final disposal), where all flows exchanged with the natural environment are accumulated and then translated into environmental impact categories (e.g., global warming and acidification). The principles and framework of LCA have been proposed by the International Standards Organization (ISO), which are generally accepted by the international community and stakeholders. According to ISO 14,040 [215,216], the framework for LCA includes (1) definition of goal and scope; (2) life cycle inventory analysis; (3) life cycle impact assessment; and (4) interpretation. Aside from ISO standard, Ellingsen, et al. [217] also described an environmental life-cycle screening framework tailored to evaluate the promising materials for batteries and their associated contributions to environmental sustainability during the life cycles of EVs.

In the first stage of LCA, several key elements should be considered, especially in dealing with energy issues, such as policy-making needs, energy penalty, scale-up challenges, non-climate environmental impacts, market effects, and uncertainty management [218]. Table 4 presents the important categories and key performance indicators for life-cycle environmental screening of LIBs for EVs. For the LCA of batteries, the commonly used functional unit is to deliver a unit of electricity (e.g., 1 kWh) via batteries [219]. For the life cycle impact assessment, metrics evaluated often include global warming potential, cumulative energy demand, human health, ecosystem quality, and resources indicators [220].

LIB technologies would generate significant environmental impacts because extensive energy and materials are consumed during the life cycle (e.g., from production to disposal). A study reported by USEPA [221] reveals that batteries with the use of Ni and Co cathodes and solvent-based electrode processing exhibit significant environmental impacts, especially on resource depletion, global warming, ecological toxicity, and human health. The largest contributing processes to these impacts are those associated with the use, processing and production of Ni/Co components.

It was estimated that, during the life cycle of current LIBs, they would consume 1141–1224 MJ-equivalent energy and generate 57–85 kg CO_2 equivalent emissions per kg battery [222]. Peters, Baumann, Zimmermann, Braun and Weil [213] also completed an overview of LCA studies for LIBs, especially focusing on battery production. The results indicated that producing 1 kWh of storage capacity was generally associated with a cumulative energy demand of 328 kWh and caused GHG emissions of 110 kg CO_2-eq [213]. Other environmental impact categories such as toxicity, acidification and resource depletion may be even more important.

A similar study on a mass-produced battery (i.e., a 24-kWh LIB) in a commercial (i.e., Ford Focus) electric vehicle revealed that the cradle-to-gate GHG emissions were about 140 kg CO_2-eq per kWh, equivalent to 11 kg CO_2-eq per kg of battery [223]. In this case, cell manufacturing was the key contributor, accounting for 45% of the GHG emissions. Dunn, Gaines, Sullivan and Wang [194] also conducted an LCA study for LIBs used in electric vehicles via the GREET model, where the system boundary included material production, battery assembly, use, and recycling. The estimated cradle-to-gate energy demand and GHG emissions were 75 MJ and 5.1 kg CO_2-eq per kg of battery, respectively. Deng, et al. [224] carried out a comprehensive LCA on a conventional battery (i.e., nickel-cobalt-manganese and graphite) and a LiSB (i.e., a graphene sulfur composite cathode and a lithium metal anode) for actual electric vehicles. The results indicated that the environmental impacts of the LiSBs were generally 9–90% lower than that of the conventional battery.

According to a comparative LCA on stationary LIB technologies [219], the key components and/or processes that would significantly pose impacts are, in decreasing order, (1) positive electrode (cathode) material, (2) negative electrode (copper) substrate, (3) battery management system (e.g., integrated circuits), (4) electricity used during manufacturing, (5) cell container (i.e., aluminum), and (6) heat (i.e., natural gas during manufacturing). A similar study on the LCA of LIBs in EVs was conducted, and it was found that adopting low-throughput assembly facilities caused the assembly stage to dominate cradle-to-gate impacts, since the energy intensity of battery assembly depends on facility throughput [196]. The energy consumption of equipment, especially the dry room, is mainly throughput independent. Apart from the energy intensity of the assembly process, cathode material production and aluminum use as a structural material were found to be the most significant contributors to environmental impacts.

The choices of material and processing in the supply chain (i.e., specific to suppliers, producers, and recyclers) would be a key contributing factor to overall environmental impacts associated with the life cycles of batteries [221]. For policy-makers, the use of higher energy density batteries with better chemical characteristics should be encouraged, since longer charge-discharge cycles in a service life would lower the environmental impacts. Yu et al. [225]

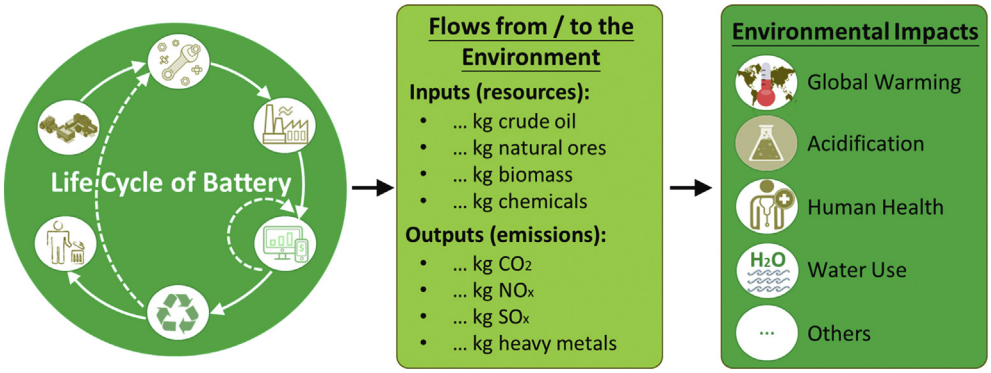

Fig. 16. General concept of LCA: The stages of the entire life-cycle for battery technologies includes raw materials extraction/acquisition, materials processing, components manufacture, product manufacture, product use, and final disposal/end-of-life.

Table 4
Important Categories and indicators for life-cycle environmental screening of LIBs for EVs.

Stages	Category	Key performance indicators
Materials (extraction)	Feedstock and energy sources	• Type of energy use (renewables) • Utilization of biomass (plant-based) • Transportation of feedstock
Production (manufacturing)	Synthesis of materials	• Structure and pore size distribution • Morphology (surface characterization) • Composition • Electrolyte formula
	Environmental intensity of materials	• Exposure risks and hazards • Scarcity • Damage to human health • Damage to ecosystems
	Material and weight efficiency	• Energy density • Power density • Synthesis material losses (yields) • Light-weighting
	Energy efficiency	• Energy of nanosynthesis
Use (service)	Electrochemical performance	• Ionic diffusion kinetics • Electrical conductivity
	Material and weight efficiency	• Lifetime (charge/discharge) • Stability
	Energy efficiency	• Device efficiency • Durability
End of life (recycling)	Material and weight efficiency Quality of product	• Recyclability • Recovery ratios • Purity of desired products • Morphology

suggested that a minimum of 200 charge-discharge cycles for secondary batteries was required to reduce the environmental impacts of LIBs. Furthermore, significant impacts on global warming potential and other environmental and human health categories were contributed from the electricity grids used to charge the batteries prior to vehicle operation [221].

4.3. Opportunities and challenges: green chemistry and technology

Today, sustainability is considered in addition to engineering performance in the design of new materials for batteries. Within this framework, the concepts of “green chemistry” and “green technology” are becoming more important than ever to establish a green supply chain for sustainable batteries. For instance, a solventless practice would lower energy consumption and potential impacts to the environment and human health, which was a common approach to green chemistry. Regarding green technologies, for example, the main constituents of biomass are among the elements which are naturally cycled within the biosphere, e.g., H, O, S, P, Na, Mg, K, Ca, Mn, Fe, and Ti [226]. These elements are in contrast to the main constituents of current LIBs (e.g., Li, Co, Ni, Cu, and F). Therefore, from the green chemistry point of view, the evolution of battery-constituting elements should shift from Li to Na (or Mg–K–Ca); from Co/Ni/Cu to Ti (or Mn–Fe); from F to Cl (or Si–S) to prepare environmentally friendly compounds [30].

Current recyclers would face no restrictions in process design, as there are no regulations regarding recycling of large-format LIBs [200]. However, recycling processes must be designed to be compliant with anticipated regulations and be flexible for a specific evolving design of chemistry. There are 12 principles of green chemistry that should be considered when designing or improving materials, products, processes and systems [217,227]. For the next generation of LIBs, the battery and its associated production should be designed for resource and material efficiency, which can be achieved through improvements in synthesis yields, light-weighting, durability, and recyclability. Attention should also be focused on indirect emissions, and pollution treatment costs should be taken account in green profit analysis [228].

Currently, EVs are powered by LIBs due to their high energy density and power density. The energy density and environmental footprint of LIBs are largely related to the physico-chemical properties of the electrodes such as nanostructure and BET surface area.

For instance, single wall carbon nanotubes (SWCNTs) exhibit an improved energy density and ultimate performance of LIBs [229]. However, the energy needed to produce the SWCNT anodes was significant due to these materials being in the early stages of development [221]. Over time, the overall environmental profile of SWCNT technology could improve dramatically once the energy intensity of the manufacturing process is significantly reduced. Furthermore, although the nanostructured electrodes (i.e., nanotechnologies) would not affect recycling yields compared with bulk materials, nanomaterials can become airborne and then pose exposure risks and hazards to workers during recycling [230]. Another green approach to developing a sustainable battery has been to replace lithium with a similar, but less hazardous material like sodium [231,232]. The abundance of a precursor (or an element) should be considered in controlling the cost of batteries. For instance, sodium is in greater abundance and has a lower risk of explosion than lithium for battery use. Singh et al. [232] developed the mineral eldfellite ($NaFe(SO_4)_2$), comprised of Na^+ and Fe^{3+} layers separated at a fixed distance by SO_4^{2-} polyhedral, as a potential material for Na-ion cathode.

5. Perspective and prospective

This review article presents a brief glimpse into advances in the synthesis of biomass-based nanostructured materials for EES applications. The focus of this article is on sharing state-of-the-art challenges and issues on plant-derived biomass materials for various energy storage applications such as batteries and supercapacitors. In this part, a perspective and prospective on the relevant fields are provided for future research direction.

5.1. Research needs and opportunities

This overview paper provides a glimpse into the use of biomass-derived materials for energy storage. We intend to demonstrate the methods and advantages of using biomass inspired by nature with energy-efficient, green, low-cost and possibly large-scale synthesis. The experimental results show that nature-derived materials have a significant influence on the performance of LIBs, LiSBs, SIBs and supercapacitors. Biomass is gradually becoming a research focus, as it is a promising strategy for making materials with generated structures having multiple contributions to the bulk properties. The concepts and results illustrated in this article will prompt researchers to join this field and help broaden the scope and impact of rechargeable batteries using biochar. From the engineering performance point of view, the lifetime of the battery should increase to at least 10 years, which is the lifetime that battery manufacturers seek to achieve. New battery structures and nano-energy systems are the key to enhancing battery performance.

From the sustainability point of view, the concepts of green chemistry and technology should be introduced in the production of batteries, such as the use of biomass materials as feedstock and/or the use of a solvent-less process. Manufacturers could reduce the overall life-cycle impacts of the battery by a number of means, including (1) carefully considering the choice of active and matrix materials, and (2) reducing the percentage of metals (especially cobalt and nickel) by mass. The recovered materials also should be incorporated in the production of the battery to maximize the use of secondary materials.

5.2. Plant-derived materials and its application in energy storage

Naturally abundant biomass is a green and alternative carbon source with many desired properties. Biological materials have inspired researchers to transfer natural structural design principles to artificially-made materials. Regarding fundamental and applied research, the focus should be on improvement of synthesis strategies, chemical modification via molecular chemistry, and construction of nanostructures. As a result, bionics would play an increasingly important role in the development of advanced functional structures. For instance, plant-derived ACs can be used as electrodes toward the construction of high-energy EES devices via cost-effective and easy preparation. After use, the spent battery can be further recycled to ensure environmental sustainability towards a circular economy system. This suggests that future research should be focused on fundamental studies and device configuration optimization with the goal to achieve a high level of sustainability. This approach requires cross-cutting collaboration among physicists, chemists and engineers from materials science, chemical engineering, environmental engineering, and economics.

5.3. Cross-disciplinary practices toward environmentally sustainable electromobility

Overcoming the challenges in current LIB technologies will require concerted efforts and a cross-disciplinary perspective that encompasses collaboration among materials science, chemical engineering, mechanical engineering and environmental management. In other words, the benefits can be realized by simultaneously incorporating nanotechnology, nanotoxicology, eco-design and green chemistry/engineering considerations. It is noted that nanotechnologies provide a broad range of opportunities to promote the technical and environmental performance of electric vehicles. However, the physico-chemical properties of novel nanomaterials may affect existing recycling and disposal processes. As a result, environmental impact assessment of battery recycling should be carefully conducted to provide a basis for system optimization. In the meantime, an improved flow of information would benefit both the environment and nanotechnology communities.

To facilitate making LIB recycling economically viable, four key elements should be considered: (1) improvement in separation technologies for efficiently recovering valuable components from cells; (2) establishment of a flexible and standardized system for battery materials and designs; (3) green design of recycling processes such as separation of cathode materials at an early stage; and (4) coordinating the relevant regulations to assure the promotion of recycling. Apart from the technological challenge perspective, sound regulations can ensure safe transport and handling of spent LIBs, deter cross-contamination, and provide economic incentives for recycling.

Acknowledgements

High appreciation goes to the Ministry of Science and Technology (MOST) of Taiwan (ROC) under Grant Number MOST 106-2119-M-002-007, and 106-3113-E-007-002 for the financial support

List of acronyms

ACs	Actived carbons
ACF	Activated carbon foam
BET	Brunnauer-Emmett-Teller
CES	Circular economy system
CE	Coulombic efficiency
CMC	Carboxymethyl cellulose
EES	Electrochemical energy storage
EVs	Electric vehicles

FHLC	Hierarchical lamellar porous carbon
FCs	Fuel cells
GHG	Greenhouse gas
HEVs	Hybrid electric vehicles
HC	Hydrochar
IC	Irreversible capacity
IEP	Isoelectric point
KOH	Potassium hydroxide
LCA	Life cycle assessment
LIBs	Lithium ion batteries
LiSBs	Lithium-sulfur batteries
MgO	Magnesium oxide
MCAs	Magnetite carbon aerogels
MPCSs	Micro-/mesoporous porous carbon spheres
PAN	Polyacrylonitrile
PVdF	Polyvinylidene difluoride
PCNS	Porous carbon nanosheets
SDG	Sustainable development goal
SIBs	Sodium ion batteries
SSA	Specific surface area
SWCNTs	Single wall carbon nanotubes

References

[1] M. Kunduraci, J. Solid State Electrochem. 20 (8) (2016) 2105.
[2] P.J. Mankowski, et al., Burns 42 (4) (2016) e61.
[3] S. Nejad, et al., J. Power Sources 316 (2016) 183.
[4] F. Pan, et al., Chem. Mater. 28 (7) (2016) 2052.
[5] B. Wang, et al., Graphene-inorganic composites as electrode materials for lithium-ion batteries, in: M. Antonietti, K. Mullen (Eds.), Chemical Synthesis and Applications of Graphene and Carbon Materials, John Wiley & Sons, Inc, 2016, p. 272.
[6] M. Armand, J.M. Tarascon, Nature 451 (7179) (2008) 652.
[7] Y. Li, et al., Renew. Sustain. Energy Rev. 74 (2017) 19.
[8] H.-W. Lee, et al., Current Opin. Chem. Eng. 12 (2016) 37.
[9] A. Doménech-Carbó, Electrochemistry of Porous Materials, CRC press, Boca Raton, FL, 2010.
[10] G. Lu, et al., Nat. Chem. 4 (4) (2012) 310.
[11] Y. Kang, T.A. Taton, J. Am. Chem. Soc. 125 (19) (2003) 5650.
[12] N. Nitta, et al., Mater. Today 18 (5) (2015) 252.
[13] N. Liu, et al., Sci. Rep. 3 (2013) 1919.
[14] L. Zhang, et al., Green Chem. 16 (8) (2014).
[15] T. Storelvmo, et al., Nat. Geosci 9 (4) (2016) 286.
[16] M. Ranson, R.N. Stavins, Clim. Pol. 16 (3) (2016) 284.
[17] M. Balat, G. Ayar, Energy Sources 27 (10) (2005) 931.
[18] I. Kovalenko, et al., Science 334 (6052) (2011) 75.
[19] M. Jensen, et al., J. Am. Chem. Soc. 131 (7) (2009) 2717.
[20] Y. Xia, et al., J. Mater. Chem. 22 (18) (2012) 9209.
[21] X. Zhao, et al., Nanoscale 3 (3) (2011) 839.
[22] J. Deng, et al., Green Chem. 18 (18) (2016) 4824.
[23] C.B. Field, et al., Science 281 (5374) (1998) 237.
[24] S.-Y. Pan, et al., Curr. Sustain. Renew. Energy Rep. 2 (4) (2015) 145.
[25] T. Kan, et al., Renew. Sustain. Energy Rev. 57 (2016) 1126.
[26] WGR, Global Lithium-Ion Battery Industry Situation and Prospects Research Report 2017, 152, Wiseguy Research Consultants, Maharashtra, 2017.
[27] Y. Xu, et al., Mater. Today (2017). In press, https://doi.org/10.1016/j.mattod.2017.07.005.
[28] Forbidden Materials and Packages, in: 49 CFR 173.21, 10-1-16 ed.; GPO 49, Government Publishing Office, 2011. CFR 173.21.
[29] S.-Y. Pan, et al., J. Clean. Prod. 108 (2015) 409.
[30] D. Larcher, J.M. Tarascon, Nat. Chem. 7 (1) (2015) 19.
[31] L. Gaines, MRS Bull. 37 (04) (2012) 333.
[32] Y. Shu, et al., Bull. Chem. Soc. Jpn. 90 (1) (2016) 44.
[33] M. Borghei, et al., Appl. Catal. B Environ. 204 (2017) 394.
[34] O.-W. Achaw, G. Afrane, Microporous Mesoporous Mater. 112 (1–3) (2008) 284.
[35] K. Sun, J.C. Jiang, Biomass Bioenergy 34 (4) (2010) 539.
[36] Y. Wen, et al., J. Alloy. Comp. 699 (2017) 126.
[37] M.K. Rybarczyk, et al., Green Chem. 18 (19) (2016) 5169.
[38] N. Yalçın, V. Sevinç, Carbon 38 (14) (2000) 1943.
[39] B. Li, et al., Energy Environ. Sci. 9 (1) (2016) 102.
[40] K. Yang, et al., Chem. Eur. J. 22 (10) (2016) 3239.
[41] B. Liu, et al., Nanomaterials 6 (1) (2016) 18.
[42] Rajeshwarisivaraj, et al., Bioresour. Technol. 80 (3) (2001) 233.
[43] H. Li, et al., Colloids Surf. Physicochem. Eng. Aspect. 489 (2016) 191.
[44] J. Zhang, et al., Electrochim. Acta 116 (2014) 146.
[45] J. Avom, et al., Carbon 35 (3) (1997) 365.
[46] F.-C. Wu, et al., J. Hazard. Mater. 69 (3) (1999) 287.
[47] S. Senthilkumaar, et al., J. Colloid Interface Sci. 284 (1) (2005) 78.
[48] A. Aygün, et al., Microporous Mesoporous Mater. 66 (2–3) (2003) 189.
[49] Q. Jiang, et al., Appl. Surf. Sci. 379 (2016) 73.
[50] X. Du, et al., Ionics 22 (4) (2016) 545.
[51] W.T. Tsai, et al., Chemosphere 45 (1) (2001) 51.
[52] H. Demiral, et al., Chem. Eng. Res. Des. 89 (2) (2011) 206.
[53] A.H. El-Sheikh, et al., J. Anal. Appl. Pyrol. 71 (1) (2004) 151.
[54] M. Molina-Sabio, F. Rodrıguez-Reinoso, Colloids Surf. Physicochem. Eng. Aspect. 241 (1–3) (2004) 15.
[55] C. Bouchelta, et al., J. Anal. Appl. Pyrol. 82 (1) (2008) 70.
[56] M. Shoaib, H.M. Al-Swaidan, Hem. Ind. 70 (2) (2016) 151.
[57] B.S. Girgis, A.-N.A. El-Hendawy, Microporous Mesoporous Mater. 52 (2) (2002) 105.
[58] D. Vamvuka, et al., Fuel 85 (12–13) (2006) 1763.
[59] M.J. Prauchner, et al., Carbon 110 (2016) 138.
[60] L. Nunes, et al., Renew. Sustain. Energy Rev. 53 (2016) 235.
[61] A. Aworn, et al., J. Anal. Appl. Pyrol. 82 (2) (2008) 279.
[62] J.A. Maciá-Agulló, et al., Carbon 42 (7) (2004) 1367.
[63] H. Teng, et al., Carbon 35 (2) (1997) 275.
[64] W. Su, et al., Carbon 41 (4) (2003) 861.
[65] Y. Li, et al., Nano Energy 19 (2016) 165.
[66] C. Chen, et al., Nano Energy 27 (2016) 377.
[67] C. Long, et al., Nano Energy 12 (2015) 141.
[68] K. Song, et al., J. Mater. Chem. A 3 (31) (2015) 16104.
[69] W. Tian, et al., J. Mater. Chem. A 3 (10) (2015) 5656.
[70] P. Cheng, et al., Carbon 93 (2015) 315.
[71] W.-H. Qu, et al., Bioresour. Technol. 189 (2015) 285.
[72] G. Xu, et al., Green Chem. 17 (3) (2015) 1668.
[73] X. Li, et al., Bioresour. Technol. 102 (2) (2011) 1118.
[74] Y.-T. Li, et al., J. Power Sources 299 (2015) 519.
[75] R. Farma, et al., Bioresour. Technol. 132 (2013) 254.
[76] M. Olivares-Marín, et al., Mater. Chem. Phys. 114 (1) (2009) 323.
[77] B. Xu, et al., Mater. Chem. Phys. 124 (1) (2010) 504.
[78] S. Kumagai, et al., Electrochim. Acta 114 (2013) 617.
[79] G.-P. Hao, et al., Adv. Eng. Mater. 3 (11) (2013) 1421.
[80] X. Du, et al., Bioresour. Technol. 149 (2013) 31.
[81] H. Peng, et al., Electrochim. Acta 190 (2016) 862.
[82] M.S. Balathanigaimani, et al., Electrochem. Commun. 10 (6) (2008) 868.
[83] A.M. Dehkhoda, et al., Biomass Bioenergy 87 (2016) 107.
[84] B. Liu, et al., Electrochim. Acta 208 (2016) 55.
[85] M.V. Lebedeva, et al., Mater. Renew. Sustain. Energy 4 (4) (2015).
[86] D. Wang, et al., J. Solid State Electrochem. 19 (2) (2014) 577.
[87] C. Peng, et al., Electrochim. Acta 87 (2013) 401.
[88] C. Peng, et al., RSC Adv. 4 (97) (2014) 54662.
[89] Y.-J. Kim, et al., Carbon 44 (8) (2006) 1592.
[90] A. Elmouwahidi, et al., Bioresour. Technol. 111 (2012) 185.
[91] X. Gu, et al., J. Mater. Chem. 3 (18) (2015) 9502.
[92] J. Jiang, et al., Energy Environ. Sci. 7 (8) (2014) 2670.
[93] M. Chen, et al., Chem. Eng. J. 313 (2017) 404.
[94] H. Wang, et al., Electrochim. Acta 188 (2016) 103.
[95] Y. Guo, et al., Mater. Chem. Phys. 74 (3) (2002) 320.
[96] S. Gao, et al., J. Mater. Chem. 2 (10) (2014) 3317.
[97] X. He, et al., Electrochim. Acta 105 (2013) 635.
[98] X. He, et al., J. Power Sources 240 (2013) 109.
[99] T.E. Rufford, et al., Electrochem. Commun. 10 (10) (2008) 1594.
[100] C. Wang, T. Liu, J. Alloy. Comp. 696 (2017) 42.
[101] X.-q. Wei, et al., New Carbon Mater. 30 (6) (2015) 579.
[102] Z.J. Zhang, et al., J. Alloy. Comp. 636 (2015) 275.
[103] K. Le Van, Thi T.T. Luong, Prog. Nat. Sci. Mater. Int. 24 (3) (2014) 191.
[104] M.A. Islam, et al., J Environ. Manage 203 (Pt 1) (2017) 237.
[105] M.A. Islam, et al., Ecotoxicol. Environ. Saf. 138 (2017) 279.
[106] N. Byamba-Ochir, et al., Appl. Surf. Sci. 379 (2016) 331.
[107] L. Lin, et al., Bioresour. Technol. 136 (2013) 437.
[108] Y. Sun, et al., J. Colloid Interface Sci. 368 (1) (2012) 521.
[109] J.M. Juárez-Galán, et al., Microporous Mesoporous Mater. 117 (1–2) (2009) 519.
[110] D. Prahas, et al., Chem. Eng. J. 140 (1–3) (2008) 32.
[111] D.-W. Kim, et al., Carbon 114 (2017) 98.
[112] Z. Hu, et al., Adv. Mater. 12 (1) (2000) 62.
[113] C.J. Coronella, et al., Hydrothermal carbonization of lignocellulosic biomass, in: Application of Hydrothermal Reactions to Biomass Conversion, Springer, 2014, p. 275.
[114] T. Adinaveen, et al., J. Mater. Cycles Waste Manag. 17 (4) (2015) 736.
[115] P. Carrott, M.R. Carrott, Bioresour. Technol. 98 (12) (2007) 2301.
[116] W. Klose, M. Wölki, Fuel 84 (7) (2005) 885.
[117] P.T. Williams, A.R. Reed, Biomass Bioenergy 30 (2) (2006) 144.
[118] E. Schröder, et al., J. Anal. Appl. Pyrol. 79 (1) (2007) 106.
[119] N. Gao, et al., Int. J. Hydrogen Energy 33 (20) (2008) 5430.
[120] R.M. Navarro, et al., Chem. Rev. 107 (10) (2007) 3952.
[121] M. Molina-Sabio, et al., Carbon 34 (4) (1996) 505.
[122] N.M. Haimour, S. Emeish, Waste Manag. 26 (6) (2006) 651.
[123] J.S. Hamada, et al., Food Chem. 76 (2) (2002) 135.
[124] B.H. Hameed, et al., J. Hazard. Mater. 141 (3) (2007) 819.
[125] X. Gu, et al., Nano Research 8 (1) (2015) 129.

[126] C.-S. Yang, et al., Curr. Appl. Phys. 14 (12) (2014) 1616.
[127] C.-a. Ma, et al., J. Power Sources 242 (2013) 273.
[128] S.-W. Han, et al., Chem. Eng. J. 254 (2014) 597.
[129] J. Jiang, et al., Adv. Mater. 24 (38) (2012) 5166.
[130] F. Su, et al., Energy Environ. Sci. 4 (3) (2011) 717.
[131] Z.S. Wu, et al., Adv. Mater. 26 (26) (2014) 4552.
[132] Z.S. Wu, et al., Adv. Mater. 24 (37) (2012) 5130.
[133] X. Wang, et al., Chem. Soc. Rev. 43 (20) (2014) 7067.
[134] R.-L. Liu, et al., Carbon 76 (2014) 84.
[135] M.G. Plaza, et al., Fuel 86 (14) (2007) 2204.
[136] G.G. Stavropoulos, et al., J. Hazard. Mater. 151 (2–3) (2008) 414.
[137] L. Zhao, et al., Carbon 48 (13) (2010) 3778.
[138] E.-J. Oh, et al., J. Power Sources 341 (2017) 240.
[139] L. Borchardt, et al., Mater. Today 20 (10) (2017) 592.
[140] K. Gong, et al., Science 323 (5915) (2009) 760.
[141] Z.-S. Wu, et al., J. Am. Chem. Soc. 134 (22) (2012) 9082.
[142] P. Chen, et al., Energy Environ. Sci. 7 (12) (2014) 4095.
[143] K.-l. Hong, et al., J. Mater. Chem. A 2 (32) (2014) 12733.
[144] A.C. Lua, J. Guo, Carbon 38 (7) (2000) 1089.
[145] N. Muhammad, et al., J. Ind. Eng. Chem. 21 (2015) 1.
[146] S. Guo, et al., Appl. Surf. Sci. 255 (20) (2009) 8443.
[147] S. Rezma, et al., Compt. Rendus Chim. 20 (9–10) (2017) 881.
[148] O.S. Amuda, et al., Biochem. Eng. J. 36 (2) (2007) 174.
[149] J. Zhang, et al., Energy Fuel 25 (5) (2011) 2187.
[150] Y. Lv, et al., J. Power Sources 209 (2012) 152.
[151] P. Nowicki, et al., J. Hazard. Mater. 181 (1–3) (2010) 1088.
[152] K. Xiao, et al., J. Mater. Chem. A 4 (2) (2016) 372.
[153] S. Pap, et al., J. Clean. Prod. 162 (2017) 958.
[154] S. Zhao, et al., RSC Adv. 7 (8) (2017) 4297.
[155] Q. Liang, et al., Nanoscale 6 (22) (2014) 13831.
[156] H. Chen, et al., Electrochim. Acta 180 (2015) 241.
[157] J.M.O. Scurlock, et al., Biomass Bioenergy 19 (4) (2000) 229.
[158] F.G. Shin, et al., J. Mater. Sci. 24 (10) (1989) 3483.
[159] X. Zhou, et al., J. Solid State Electrochem. 16 (3) (2012) 877.
[160] D. Kalderis, et al., Bioresour. Technol. 99 (15) (2008) 6809.
[161] S.K. Ramamoorthy, et al., Polym. Rev. 55 (1) (2015) 107.
[162] P.K. Malik, Dyes Pigments 56 (3) (2003) 239.
[163] C. Moreno-Castilla, et al., Carbon 39 (9) (2001) 1415.
[164] Y. Yao, F. Wu, Nano Energy 17 (2015) 91.
[165] D. Di Lecce, et al., Green Chem. 19 (15) (2017) 3442.
[166] Z. Li, et al., Energy Environ. Sci. 6 (3) (2013) 871.
[167] J.C. Arrebola, et al., J. Electrochem. Soc. 157 (7) (2010) A791.
[168] A.M. Stephan, et al., Mater. Sci. Eng. A 430 (1–2) (2006) 132.
[169] E. Unur, et al., Microporous Mesoporous Mater. 174 (2013) 25.
[170] Z. Gao, et al., Mater. Res. Lett. 5 (2) (2016) 69.
[171] W. Xing, et al., J. Electrochem. Soc. 143 (10) (1996) 3046.
[172] X. Yi, et al., Electrochim. Acta 232 (2017) 550.
[173] N. Moreno, et al., Carbon 70 (2014) 241.
[174] J. Guo, et al., Electrochim. Acta 176 (2015) 853.
[175] K. Yang, et al., Microporous Mesoporous Mater. 204 (2015) 235.
[176] S. Zhang, et al., J. Mater. Chem. 2 (38) (2014) 15889.
[177] H. Ye, et al., J. Mater. Chem. 1 (22) (2013) 6602.
[178] W. Zhou, et al., ACS Nano 7 (10) (2013) 8801.
[179] S.H. Chung, A. Manthiram, ChemSusChem 7 (6) (2014) 1655.
[180] H.S. Ryu, et al., J. Mater. Chem. 1 (5) (2013) 1573.
[181] B. Zhang, et al., ACS Appl. Mater. Interfaces 6 (15) (2014) 13174.
[182] F. Chen, et al., Electrochim. Acta 192 (2016) 99.
[183] A.M. Puziy, et al., Carbon 40 (9) (2002) 1493.
[184] Y. Li, et al., J. Mater. Chem. A 3 (1) (2015) 71.
[185] Y. Shao, et al., Nano Lett. 13 (8) (2013) 3909.
[186] X.-L. Wu, et al., ACS Nano 7 (4) (2013) 3589.
[187] Z.A. Al-Othman, et al., Chem. Eng. J. 184 (2012) 238.
[188] Z. Fan, et al., Mater. Lett. 101 (2013) 29.
[189] L. Wang, et al., ChemSusChem 6 (5) (2013) 880.
[190] Z. Zhu, et al., Sci. Rep. 5 (2015) 15936.
[191] A.M. Abioye, F.N. Ani, Renew. Sustain. Energy Rev. 52 (2015) 1282.
[192] J.M. Nabais, et al., Bioresour. Technol. 102 (3) (2011) 2781.
[193] K. Linnenkoper, A new reality for car battery recycling, Recycl. Int. (2016) 1.
[194] J.B. Dunn, et al., Environ. Sci. Technol. 46 (22) (2012) 12704.
[195] A.R. Kamali, Green Chem. 18 (7) (2016) 1952.
[196] J.B. Dunn, et al., Energy Environ. Sci. 8 (1) (2015) 158.
[197] L. Li, et al., J. Power Sources 233 (2013) 180.
[198] L. Unterreiner, et al., Energy Procedia 99 (2016) 229.
[199] B. Swain, Separ. Purif. Technol. 172 (2017) 388.
[200] L. Gaines, Sustain. Mater. Technol. 1–2 (2014) 2.
[201] P.K. Choubey, et al., Miner. Eng. 110 (2017) 104.
[202] X. Mönnighoff, et al., J. Power Sources 352 (2017) 56.
[203] L.-P. He, et al., ACS Sustain. Chem. Eng. 5 (1) (2017) 714.
[204] S. Heinrichs, et al., Recovery of NF-metal from bottomash's fine fraction: state-of-the-art in Germany, in: The 4th International Symposium on Energy from Biomass and Waste, Venice, 2012.
[205] J. Chen, et al., Green Chem. 18 (8) (2016) 2500.
[206] H. Zou, et al., Green Chem. 15 (5) (2013).
[207] E. Gratz, et al., J. Power Sources 262 (2014) 255.
[208] C. Hanisch, et al., Recycling of Lithium-Ion Batteries, in: Handbook of Clean Energy Systems, John Wiley & Sons, Ltd., 2015.
[209] W. Gao, et al., Environ. Sci. Technol. 51 (3) (2017) 1662.
[210] L. Gaines, Lithium-Ion Battery Recycling and Life Cycle Analysis, vol. 2017, Energy Systems Division, Argonne National Laboratory, USA, 2015.
[211] J.B. Dunn, et al., Material and Energy Flows in the Production of Cathode and Anode Materials for Lithium Ion Batteries, Argonne National Laboratory, USA, 2015.
[212] M. Bigum, et al., Resour. Conserv. Recycl. 122 (2017) 251.
[213] J.F. Peters, et al., Renew. Sustain. Energy Rev. 67 (2017) 491.
[214] H.A.U. de Haes, R. Heijungs, Appl. Energy 84 (7–8) (2007) 817.
[215] International Organization for Standardization, ISO 14044 — environmental management – life cycle assessment: requirements and guidelines, in: Management Environnemental — Principles, Switzerland, 2006. Vol. ISO 14040:2006(E).
[216] International Organization for Standardization, ISO 14040 — environmental management — life cycle assessment: principle and framework, in: Management Environnemental — Exigencies, Switzerland, 2006.
[217] L.A. Ellingsen, et al., Nat. Nanotechnol. 11 (12) (2016) 1039.
[218] P.-C. Chiang, S.-Y. Pan, System analysis, in: Carbon Dioxide Mineralization and Utilization, Springer Nature, Singapore, 2017, p. 187.
[219] M. Hiremath, et al., Environ. Sci. Technol. 49 (8) (2015) 4825.
[220] E. Olivetti, et al., Life Cycle Impacts of Alkaline Batteries with a Focus on End-of-life, Massachusetts Institute of Technology, USA, 2011.
[221] USEPA, Application of Life-Cycle Assessment to Nanoscale Technology: Lithium-ion Batteries for Electric Vehicles, United States Environmental Protection Agency, USA, 2013.
[222] B. Li, et al., Environ. Sci. Technol. 48 (5) (2014) 3047.
[223] H.C. Kim, et al., Environ. Sci. Technol. 50 (14) (2016) 7715.
[224] Y. Deng, et al., J. Power Sources 343 (2017) 284.
[225] Y. Yu, et al., Int. J. Environ. Res. Publ. Health 11 (3) (2014) 3185.
[226] K. Bousdira, et al., Revue des Energies Renouvelables SIENR'14 Ghardaïa, 2014, p. 99.
[227] L. Gaines, J. Sullivan, in: How Green is Battery Recycling. ANL, Argonne National Laboratory, USA, 2012, p. 2.
[228] X. Tian, et al., J. Clean. Prod. 144 (2017) 142.
[229] M. Kumar, Mater. Res. Bull. 91 (2017) 148.
[230] C. Som, et al., Toxicology 269 (2–3) (2010) 160.
[231] A. Baker, With green chemistry the potential for better batteries is charged with opportunity, in: Green Chemistry: the Nexus Blog, vol. 2017, American Chemical Society, USA, 2016.
[232] P. Singh, et al., Energy Environ. Sci. 8 (10) (2015) 3000.

Dr. Mengyao Gao is a Postdoctoral Research Fellow at Department of Chemical Engineering, National Taiwan University (NTU). She received her Ph.D. in Materials Science and Engineering from Beijing University of Chemical Technology (BUCT) in 2016. Prior to joining NTU, she worked as a visiting scholar at Chemical Science and Engineering (CSE) Division, Argonne National Laboratory, USA. Her research is mainly focused on green energy, biomass-based porous carbon materials, nanomaterials design and fabrication, and electrochemical energy storage, especially lithium batteries and stretchable devices.

Dr. Shu-Yuan Pan is a Research Associate in Carbon Cycle Research Center (CCRC), National Taiwan University (NTU). He received his Ph.D. degree in environmental engineering from NTU in 2016. He was named the Green Talents of the Year (2013) by the Federal Ministry of Education and Research (BMBF) of Germany. He had worked as a visiting scholar in RWTH Aachen University, Germany in 2014, and Argonne National Laboratory, USA in 2015. He is a Professional Engineer in environmental engineering licensed in Taiwan. His current interests include life cycle assessment, electrokinetic desalination, clean coal technology., and sustainable development.

Dr. Wen-Chang Chen is the Dean of the College of Engineering, Director of the Center for Strategic Materials Alliance for Research and Technology, and Distinguished Professor in the Department of Chemical Engineering and the Institute of Polymer Science and Engineering at National Taiwan University (NTU). He received a PhD degree in Chemical Engineering from University of Rochester in 1993 and then served as a research scientist at the Industrial Technology Research Institute of Taiwan from 1993 to 1996. He joined NTU as an Associate Professor in 1996 and was promoted to a full professor in 2000. His current research activities include electronic and optoelectronic polymers, block copolymers, and hybrid materials. He has co-authored 337 refereed articles and holds 46 issued patents.

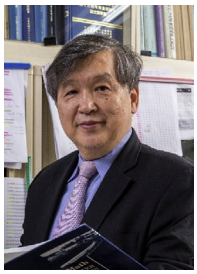

Dr. Pen-Chi Chiang is a Distinguished Professor of Graduate Institute of Environmental Engineering, National Taiwan University (NTU), and a Director of Carbon Cycle Research Center of NTU. He obtained his Ph.D. degree in Civil Engineering from Purdue University in 1982. He has worked on establishment of policies and strategies for deploying sustainable development and green technology in Taiwan. His current interests include green infrastructure, green building, healthy watershed management, cleaner production, CO_2 capture and utilization, and energy-efficient water purification technologies. He has published more than 220 SCI papers in the above areas since 1990.